



**A SOCIO-ECOLOGICAL APPROACH TO COMBAT  
DESERTIFICATION FOR SUSTAINABLE FUTURE**

# **EcoFuture**

## **Work Package 3**

### **Deliverable 3.1 Hydrologic Modeling of the JV**

Nikolaos Nikolaidis, Antonia Maragkaki, Evelina Koukianaki, Maria Lili, Sofia  
Nerantzaki (Technical University of Crete)

March 2025



**Project no.** 2243

**Project acronym:** EcoFuture

**Project title:** A socio-ecological approach to combat desertification for a sustainable future

**Call:** PRIMA Call 2022 Section 1 NEXUS WEFE IA

**Start date of project:** 01.04.2023

**Duration:** 36 months

**Deliverable title:** Hydrologic Modeling of the JV

**Due date of deliverable:** M16

**Project Coordinator:** Nikolaos Nikolaidis

**Organisation name of lead contractor for this deliverable:** Technical University of Crete (TUC)

**Lead Authors** Nikolaos Nikolaidis, Antonia Maragkaki, Evelina Koukianaki, Maria Lili, Sofia Nerantzaki

**Email** nikolaos.nikolaidis@enveng.tuc.gr

**Contributions from** Abeer Albalawneh, David Lehrer, Shaddad Attili

**Internal Reviewer 1** Maram al Naimat

**Internal Reviewer 2** Mudabr Mohammad

Dissemination level			
PU	Public/ Confidential		PU
History			
Version	Date	Reason	Revised by
01	20/7/2024	Draft	Nikolaos Nikolaidis, Antonia Maragkaki, Evelina Koukianaki
02	28/7/2024	Review	Maram al Naimat, Mudabr Mohammad
03	31/7/2024	Final	Nikolaos Nikolaidis
04	28/3/2025	Revision after Mid-term review	Sofia Nerantzaki and Nikolaos Nikolaidis

## Table of Contents

<b>List of figures</b> .....	3
<b>List of tables</b> .....	4
<b>Executive Summary</b> .....	5
<b>1. Introduction</b> .....	6
1.1 Objective.....	6
1.2 Area description .....	6
1.3 Geology, land use and soils .....	7
1.4 Climate.....	8
1.5 Water resources .....	9
1.5.1 Surface resources.....	9
1.5.2 Groundwater resources .....	10
<b>2. Methodology</b> .....	12
2.1 Model set up.....	12
2.1.1 Input data of QSWAT .....	12
2.2 Methodology .....	21
2.2.1 Model Calibration and Sensitivity Analysis.....	23
<b>3. Results</b> .....	27
<b>4. Conclusions</b> .....	38

## List of figures

Figure 1. Study area, a) JV western region, b) JV eastern region. On the western side, the Israeli area is located above the dashed line and the Palestinian region is below the dashed line.....	7
Figure 2. Geology of Jordan. The area in circle is the study area (Jreisat, K. and Yazjeen, T., 2013).....	8
Figure 3. Water Allocation Scheme for the Jordanian, Israeli and Palestinian part of the JV. Abbreviations: MCM/yr, Million Cubic Meters per year; GW, groundwater; WWTP, Wastewater Treatment Plant; NRW, Non-Revenue Water; KAC, King Abdullah Canal. ....	11
Figure 4. Input and Output data of QSWAT .....	12
Figure 5. Available Precipitation stations .....	13
Figure 6. Available Temperature stations.....	14
Figure 7. Available CFSR stations .....	14
Figure 8. DEM of case study.....	17
Figure 9. Soil Type of case study .....	17
Figure 10. Land Uses of case study .....	18
Figure 11. Available Dams in the case study.....	19

Figure 12. Fluctuation of the annual inflow of the dams (MCM) .....	20
Figure 13. Model setup with subbasins and available Dams in the case study.....	20
Figure 14. Selected Precipitation stations .....	21
Figure 15. Selected Temperature stations.....	22
Figure 16. Calibration points.....	24
Figure 17. Comparison of observed and simulated daily flow data at the Yavneal hydrometric station. .	27
Figure 18. Comparison of observed and simulated daily flow data at the Jordan Near Old Bridge hydrometric station. ....	28
Figure 19. Comparison of observed and simulated monthly flow data at the Harod hydrometric station. .....	29
Figure 20. Comparison of observed and simulated daily flow data at the Tavor hydrometric station.....	30
Figure 21. Comparison of observed and simulated monthly flow data at the Yarmouk hydrometric station. ....	30
Figure 22. Comparison of observed and simulated daily flow data at the Faria hydrometric station. ....	31
Figure 23. Comparison of observed and simulated daily flow data at the Faria hydrometric station .....	32
Figure 24. Comparison of observed and simulated daily flow data at the Jordan Baptism Site hydrometric station. ....	33
Figure 25. Comparison of observed and simulated annual flow data at the Jordan Baptism Site hydrometric station .....	33
Figure 26. Variability of weighted average precipitation and evapotranspiration in the western Jordan Valley.....	37
Figure 27. Variability of weighted average precipitation and evapotranspiration in the eastern Jordan Valley.....	37
Figure 28. Average Annual Inflow and Outflow of the Jordan River for 2000-2021 .....	37

## List of tables

Table 1. Total number of available stations for Precipitation and Temperature for each organization ....	13
Table 2. Percent Land Use Categories .....	18
Table 3. Soil Types and Their Respective Percentages .....	19
Table 4. Characteristics of selected precipitation stations .....	22
Table 5. Characteristics of selected temperature stations .....	23
Table 6. Annual flow in million cubic meters (MCM) of calibration points .....	25
Table 7. QSWAT parameters used for sensitivity analysis.....	26
Table 8. T-values (p-values) of the most significant parameters (p-value < 0.05) for every sub-basin with available hydrological data .....	34
Table 9. Comparison of observed and simulated flow in MCM of calibration points. ....	35
Table 10. Weighted average precipitation and potential evapotranspiration for each year.....	36

## Executive Summary

The objective of this task is to evaluate the available water resources in the JV. The hydrologic model QSWAT was used. The QSWAT is a watershed-based model that accounts for the spatial variability of the watershed by subdividing it into sub-catchments. Within each sub-catchment it specifies what is referred to as Hydrologic Response Units (HRUs). Each HRU is a combination of land use, soil and slope and is defined vertically from the vegetation to shallow and deep aquifers. QSWAT has been used extensively to simulate impacts from agricultural practices, point and nonpoint sources of pollution including urban areas. In addition, it has been used to evaluate land use management practices and spatial improvement measures such as filter strips and riparian buffers. Historical, precipitation, meteorological and hydrologic flow data were used to calibrate the model for the JV.

The hydrologic system of the Jordan valley is heavily modified with many reservoirs, canals and pumping stations that divert water for irrigation and drinking water supply. Heavily modified hydrologic systems require detailed daily time series of flow data for the inflow and outflow from the reservoirs as well as water abstractions and diversions which are not available for the Jordan Valley basin. Especially for the Yarmouk River, there are many dams controlling the flow in Syria with no available data. In addition, the distribution of precipitation and meteorological stations is uneven with significant gaps. Finally, there are very few hydrometric stations in Jordan River and its tributaries with insufficient time series for proper hydrologic calibration of the area.

The lack of available data as well as the presence of a complex and insufficiently documented management system for water availability and distribution in the study area, coupled with conflicting information regarding available water supplies and extractions, currently renders precise and detailed modeling of the area unattainable. The collection of data in all three territories became extremely difficult due to the ongoing war in Gaza.

Given the above limitations, the hydrologic calibration was conducted for the Jordan valley area (after the Jordanian Dams) and the aim was to capture the flow patterns and quantity of the Jordan River before it enters the Dead Sea and establish an average hydrologic budget for the JV.

Based on the hydrologic simulation for the years 2000-2021 the following hydrologic budget for the Jordan Valley was estimated. The total area simulated is 4225 km<sup>2</sup>, the annual average areal weighted precipitation was 290 mm and the annual average areal weighted ET 200 mm. This translates into 1225 Mm<sup>3</sup>/yr of precipitation volume and 845 Mm<sup>3</sup>/yr volume of ET. The available water is the difference 380 Mm<sup>3</sup>/yr of which 121 Mm<sup>3</sup>/yr is the average outflow of Jordan river to the Dead Sea. In addition, the groundwater abstraction has been estimated to 146 Mm<sup>3</sup>/yr in the three territories (not accounting for the pumping in area C of the Palestinian territory).

The available water resources in the JV are extremely limited and are expected to decline due to climate change with significant impact on the ecosystem and the biodiversity as well as the available water supply to cover the demand for drinking water and agriculture.

## 1. Introduction

### 1.1 Objective

The objective of this task is to evaluate the available water resources in the JV using the hydrologic model QSWAT. The QSWAT is a watershed-based model that accounts for the spatial variability of the watershed by subdividing it into sub-catchments. Within each sub-catchment it specifies what is referred to as Hydrologic Response Units (HRUs). Each HRU is a combination of land use, soil and slope and is defined vertically from the vegetation to shallow and deep aquifers. QSWAT has been used extensively to simulate impacts from agricultural practices, point and nonpoint sources of pollution including urban areas. In addition, it has been used to evaluate land use management practices and spatial improvement measures such as filter strips and riparian buffers. Historical, precipitation, meteorological and hydrologic flow data were used to calibrate the model for the JV. Once the model was calibrated, the available water in every sub-basin was estimated as well as future scenarios of climate change were simulated in order to assess the impact of climate change on water availability as part of Task 3.5. The report contains the hydrologic simulation of the JV and the estimation of available water in each country (Jordan, Palestine, Israel).

### 1.2 Area description

The area of interest consists of the Jordanian, the Israeli and the Palestinian side of the JV (Figure 1). The Jordanian side of the JV is an area that extends from the Sea of Galilee in the north to the Dead Sea in the south. The Jordan Depression runs from Wadi Araba to the Dead Sea and forms part of the Rift Valley that extends from North Syria to East Africa. It rises from the Gulf of Aqaba over about 80 km up to about 250 m a.s.l, then drops gently towards the Dead Sea (419 m b.s.l), and then rises from 419 m b.s.l to 210 m b.s.l at Lake Tiberias.

The JV is about 104 km long, its width varies from 4 to 16 km between the Jordan River and the East Mountains chain. The valley is divided into three distinct areas: the Northern JV, the Middle JV, and the Southern JV. Each area is examined with a resolution that captures the specific hydrological and agricultural characteristics intrinsic to its locale. The Northern section encompasses the regions around the Yarmouk River basin and extends to the lush, water-rich areas near the Sea of Galilee. The Middle segment includes the Deir Alla region, where the Jordan River meanders through central areas with distinct agricultural practices and water management challenges. Lastly, the Southern part covers the arid regions around the South Shouna, where water scarcity presents unique issues for sustainable resource management.

The area in the western and eastern side of the JV is 1,574 and 1,343 km<sup>2</sup> respectively. The Israeli area is located north of the dashed line and the Palestinian area is south of the dashed line (Figure 1a). The Israeli part, above the dashed line is 693 km<sup>2</sup>. The Palestinian territory of the JV is divided according to the “Oslo Accords” into:

- Area A, which is under Palestinian jurisdiction. This area is 85 km<sup>2</sup> and includes Jericho and the surrounding area (7.4% of the total area of the JV),
- Area B, which is a joint sharing area between the Authority and Israel, has an area of 50 km<sup>2</sup> (4.3% of the total area of the JV),
- Area C, which is under full Israeli control, has an area of 1,155 km<sup>2</sup> (88.3% of the total area of the JV).

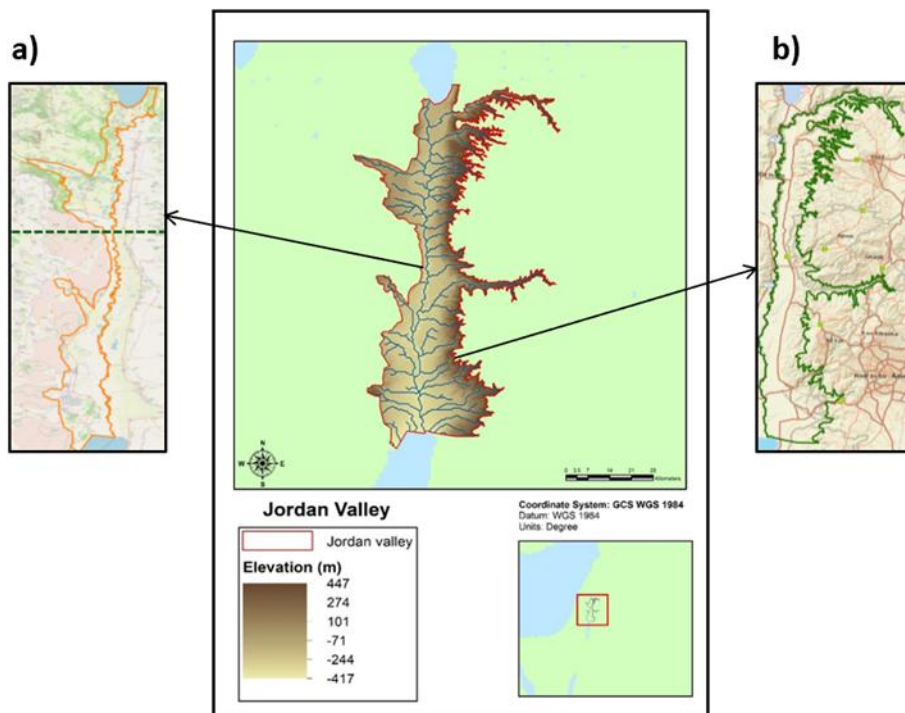


Figure 1. Study area, a) JV western region, b) JV eastern region. On the western side, the Israeli area is located above the dashed line and the Palestinian region is below the dashed line.

### 1.3 Geology, land use and soils

The mountains located in the highlands primarily consist of sedimentary rocks. The JV is comprised of non-consolidated alluvial sediments of gravel, sand, shale and clay deposits (Figure 2). The salty deposits, clay and shale, have been eroded from the hills of the valley and deposited thousands of years ago. The valley plateau was recently deposited and established a fertile area used for agricultural purposes. In areas of the valley such as Adasiya, Mukheiba, North Shouna and Katar, Basalts are found. The groundwater abstraction occurs from Quaternary sand, gravel and escarpments in the JV and, Cretaceous limestone and basalt in the Jordan highland (Suleiman, 2003).

The topographic nature of the area is characterized by the typical rift valley feature. Over short distances from the edges of the valley the elevation abruptly declines and closer towards the Jordan River it drops more gently. Alongside the valley, the elevation declines from north to south. In the northern part of the

valley the elevation decreases by 375 m over 10 km. In the middle part of the valley the elevation decline exceeds 500 m over 9 km. In the very south, this drop reduces to 100 m over 8 km (Kool, 2016).

The study area has a total surface area of 2,256 km<sup>2</sup>. A total of 1,389 km<sup>2</sup> is uncultivated land accounting for 61.5% of the total area. The area used for agricultural purposes accounts for 32% (716.8 km<sup>2</sup>) of the total surface area and the built-up area is 80.6 km<sup>2</sup> (3.6%). Wadis, fish farming and reservoirs have a surface area of 43.2, 20 and 6.4 km<sup>2</sup> accounting for 1.7, 0.9 and 0.3% of the total area respectively.

The dominant soil types are regosols, rendzinas and serozems, which are mainly tertiary deposits, and to a lesser extent lithosols, all of them suitable for cultivation. As a result, most of the land in the area that can be provided with water is used for agriculture and horticulture (Kool, 2016).

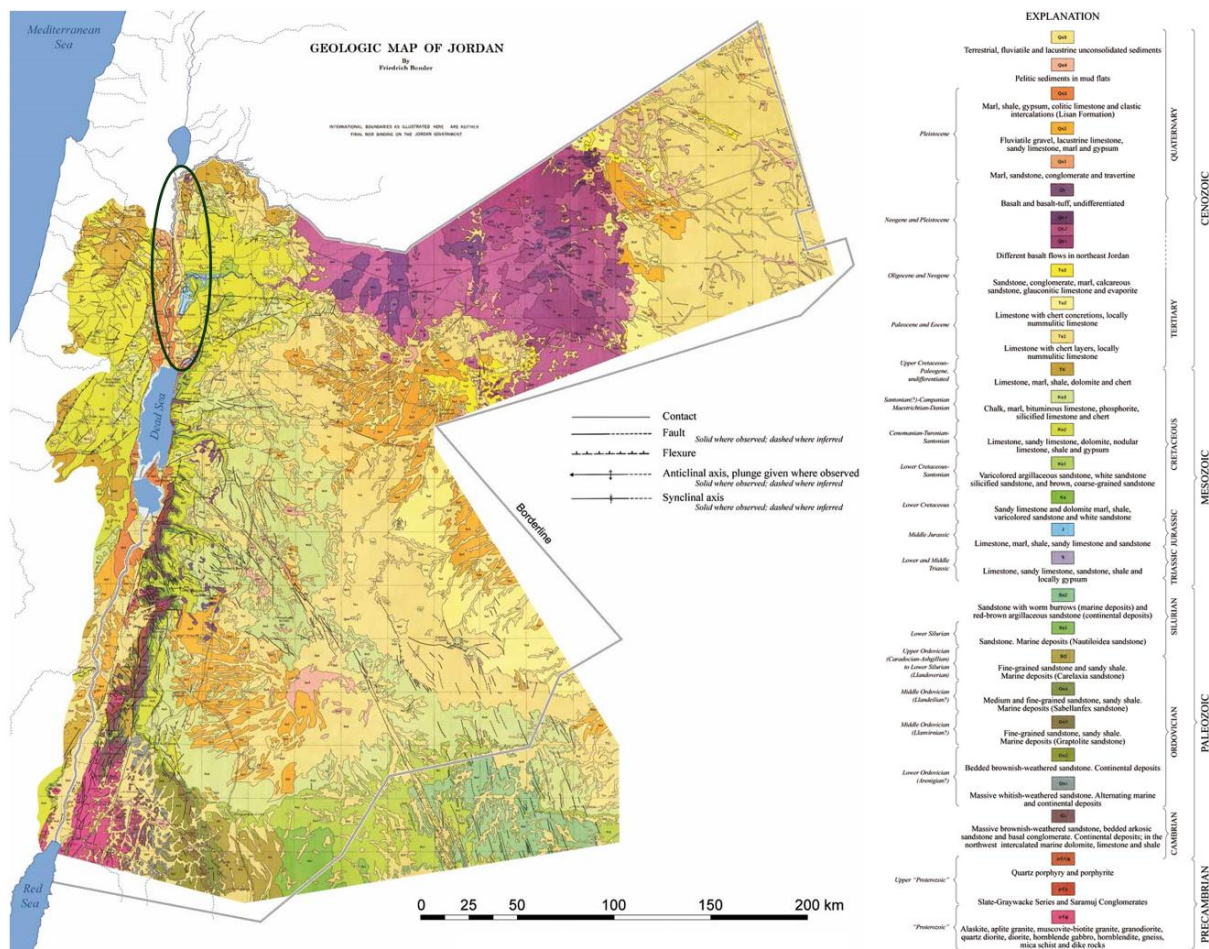


Figure 2. Geology of Jordan. The area in circle is the study area (Jreisat, K. and Yazjeen, T., 2013).

## 1.4 Climate

The JV presents climatic variability from the north to the south and from the east to the west. It has a semi-arid climate, characterized by hot dry summers and mild wet winters. However, moving southward

through the valley towards the Dead Sea the climate becomes more arid. The daily average temperature ranges between 15°C and 22°C from November to March and between 30°C and 33°C in the summer. Snowfall and frost are extremely rare and are only observed once or twice a year in the zones with altitude higher than 700 m.

The rainy season begins in October and lasts until April/May. The bulk of precipitation occurs during the months December through February/March. Precipitation fluctuates significantly from the north to the south of the valley. In the northern areas the annual precipitation can exceed 600 mm and in the southern areas annual precipitation is less than 70 mm. During dry years, the northern parts of the valley may receive only 200 mm, while areas on the shores of the Dead Sea may receive less than 100 mm (Kool, 2016; Suleiman, 2003).

## 1.5 Water resources

### 1.5.1 Surface resources

The major water sources in the JV are the Jordan River, the Lake of Tiberias (or Sea of Galilee) and the Yarmouk and Zarqa rivers. Lake Tiberias is the largest surface freshwater reservoir in the region. The Lower part of the Jordan River originates from the Sea of Galilee. Historically, the Lower Jordan River received around 600 MCM/yr from the Sea of Galilee and about 470 MCM/yr from the Yarmouk River. Additional inflow from Zarqa River and nine major Jordanian streams entering the valley from east, resulted in an outflow of 1,250 MCM/yr into the Dead Sea. Due to water diversion projects the outflow has decreased to 40-100 MCM/yr (Royal HaskoningDHV and MASAR, 2020).

The Yarmouk River is the main water source of the King Abdullah Canal (KAC), which carries water for irrigating crops in the JV and for domestic use in Amman. Moreover, water from Yarmouk River is diverted by dams, including the Wehdah dam (or Unity Dam) which is located at the border with Syria. KAC has a total length of 110 km and receives water from Lake Tiberias and a discharge from King Talal Dam (KTD), which is a mix of freshwater from the Zarqa River and effluent from the As Samra wastewater treatment plant (WWTP).

KAC includes two sections: a) North KAC and b) South KAC (Figure 3). North KAC is 65 km long and receives water from Yarmouk River, Wehdah and Kufranja dams, Mukheiba Wells, the KAC conveyor (water supplied from Lake Tiberias under the Peace Treaty since June 1995), and the side Wadis (Wadi Al-Arab, Wadi Jurum, Wadi Yabis, Wadi Rajib) whenever water is available. More specifically, North KAC receives 50.5 MCM/yr from Lake Tiberias, 42.8 MCM/yr from Wehdah dam, 23.3 MCM/yr from Mukheiba wells, 15.1 MCM/yr from Yarmouk/DS Wehdah dam, 5 MCM/yr from Kufranja dam, 3.1 MCM/yr from Wadis (1.3 from Wadi Jurum, 0.9 from Wadi Al-Arab, 0.5 from Wadi Rajib, 0.4 from Wadi Yabis). North KAC provides water for irrigation in North Shouna (73 MCM/yr), drinking water in Amman (66.1 MCM/yr) and returns water to Wadi Al-Arab dam (9.1 MCM/yr).

South KAC is 45 km long and obtains water from As Samra WWTP (118 MCM/yr), KTD (59 MCM/yr), several WWTPs (WWTP Al Baqaa: 5.8 MCM/yr, WWTP Wadi Al Seer: 3.5 MCM/yr, WWTP As Salt: 2.8 MCM/yr, WWTP Fuheis: 1.5 MCM/yr, WWTP Kufranja: 1.4 MCM/yr) and KAC North (3.4 MCM/yr). South KAC

provides water for irrigation in Deir Alla (52 MCM/yr) and South Shouna (81 MCM/yr) and to the Karama Dam (1.3 MCM/yr) which stores winter water (Al Absi et al., 2020; Royal HaskoningDHV and MASAR, 2020; NARC).

For the Israeli part of the JV, the freshwater supply system is mixed. The National Water Carrier (NWC) supplies Israel with drinking water (7.1 MCM/yr) that originates from Tiberias Lake in the north and desalinated water. In addition, the NWC provides 70.9 MCM/yr of freshwater which is mixed with 6.9 MCM/yr treated wastewater and it is used for irrigation (in total 67.8 MCM/yr).

For the Palestinian part of the JV, Mekorot, the Israel Water Company supplies water which is mixed with water from wells, and it is used for domestic consumption (6.4 MCM/yr). Lastly, groundwater, harvested rainwater and treated wastewater (0.7 MCM/yr) are used for irrigation purposes in Palestine (32.8 MCM/yr).

### 1.5.2 Groundwater resources

The groundwater system in the JV consists of various aquifers from different geological ages. The depth of groundwater aquifers in Jordan varies depending on the location and geological characteristics of the area. In some regions, aquifers may be shallow (a few meters), while in others, they may be deeper underground (several hundred meters). Figure 3 presents the water allocation system in the 3 territories in the JV.

At the northern JV there are 121 wells of which 70 are governmental and the 51 are private used for agriculture. The active wells in 2016 were 5 and 0.53 MCM of water was abstracted in total. At the southern JV there are 1,174 wells (117 governmental; 1,057 private wells for agricultural use) and the active wells identified in 2016 were 301 with a total abstraction of 11.2 MCM (WIT, 2018). Over the past decades, production from local wells and springs has been declining due to over abstraction (Tech, 2020). In addition, overuse has affected groundwater quality leading to high salinity and heavy metals content (Al Absi et al., 2020).

Precisely, at the Jordanian side of the JV and especially North Shouna receives groundwater from Wadi Al-Arab (2.5 MCM/yr), Shaq Al Bared (2.2 MCM/yr), Mkaimnat-Kraimeh (2.2 MCM/yr) and Tabaqet Fahel (2 MCM/yr). Deir Alla receives groundwater from Wadi Rajib (2.6 MCM/yr), Abu Ezzeighan (2.3 MCM/yr) and As Samaheyat (0.8 MCM/yr). South Shouna receives groundwater from private wells (4 MCM/yr), Zara Maeen (2.4 MCM/yr) and Kafrein (2.4 MCM/yr). These groundwater sources are used as drinking water for these regions.

Israeli settlements control more than 50% of the total groundwater abstractions in the West Bank. Mekorot, the Israeli water company, provides 75 MCM/yr of water to settlements in the West Bank, with 44 MCM/yr sourced from wells controlled by Israel within the West Bank. Israel operates 42 abstraction wells within the West Bank, all owned and operated by Mekorot. These wells are predominantly drilled in the Eastern Aquifer in the JV, with a collective capacity of 56.9 MCM/yr. At the Israeli side of the JV, 67 MCM/yr of groundwater is used in aquaculture which is 50% of the total irrigation water. At the Palestinian side of the JV, groundwater is used for both irrigation and domestic use.



## 2. Methodology

### 2.1 Model set up

#### 2.1.1 Input data of QSWAT

For the operation of the QSWAT model, various types of data are required, including meteorological data daily and geospatial data such as land use, soil type, and the Digital Elevation Model (DEM). The outputs of QSWAT include evapotranspiration, total flow, surface flow, and infiltration (Figure 4). QSWAT can generate these outputs on daily, monthly, or yearly intervals. The organizations providing this data include the Israel Meteorological Service (IMS), Pakistan Meteorological Department (PMD), National Aeronautics and Space Administration (NASA), Water Authority of Jordan (WAJ), the Food and Agriculture Organization Global Land Cover-SHARE (FAO GLC-SHARE), Center for Hydrometeorology and Remote Sensing (CHRS) and National Agricultural Research Center (NARC). Table 1 presents the total number of available stations for Precipitation and Temperature of each organization. Figures 5 and 6 present the spatial distribution of available Precipitation and Temperature stations. QSWAT, as shown in Figure 4, also needs statistical meteorological parameters for the case study in order to fill potential gaps in the record. These parameters were obtained from the global database that QSWAT provides (CFSR)(Figure 7).

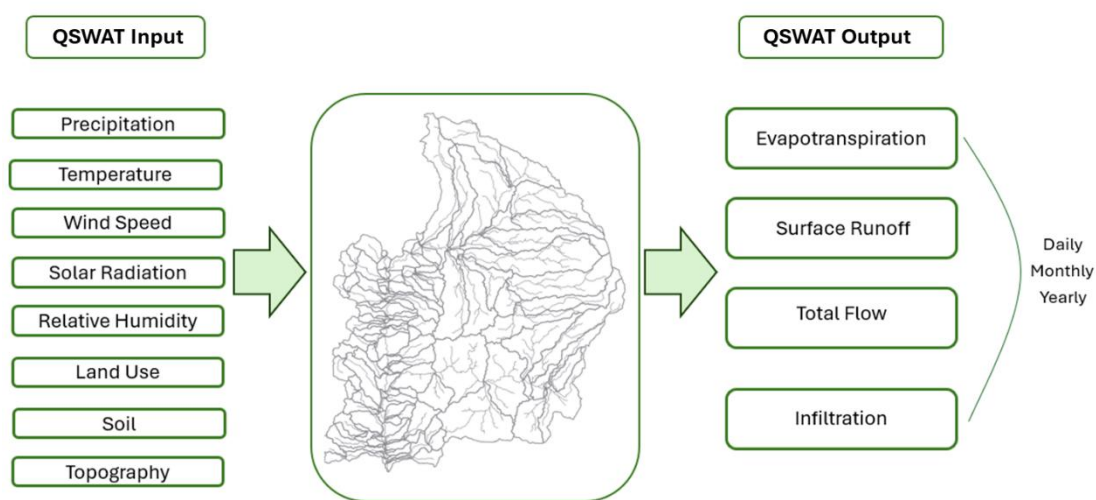


Figure 4. Input and Output data of QSWAT

Table 1. Total number of available stations for Precipitation and Temperature for each organization

Organizations	Number of Precipitation stations	Number of Temperature stations	Number of Station with statistical meteorological data
CHRS	121	0	0
IMS	452	119	0
NARC	4	3	0
NASA	3	4	0
PMD	1	1	0
WAJ	3	3	0
CFSR	0	0	20

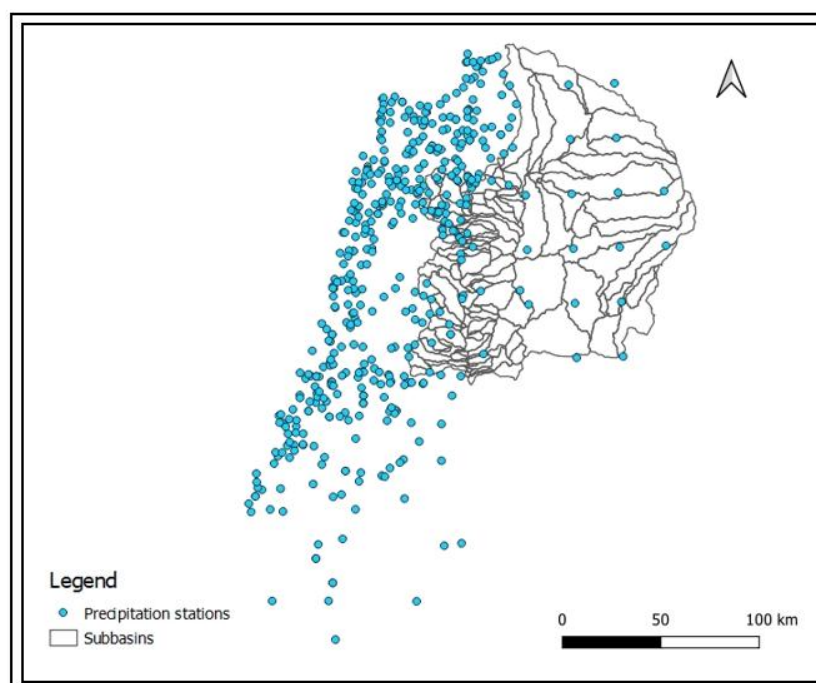


Figure 5. Available Precipitation Stations

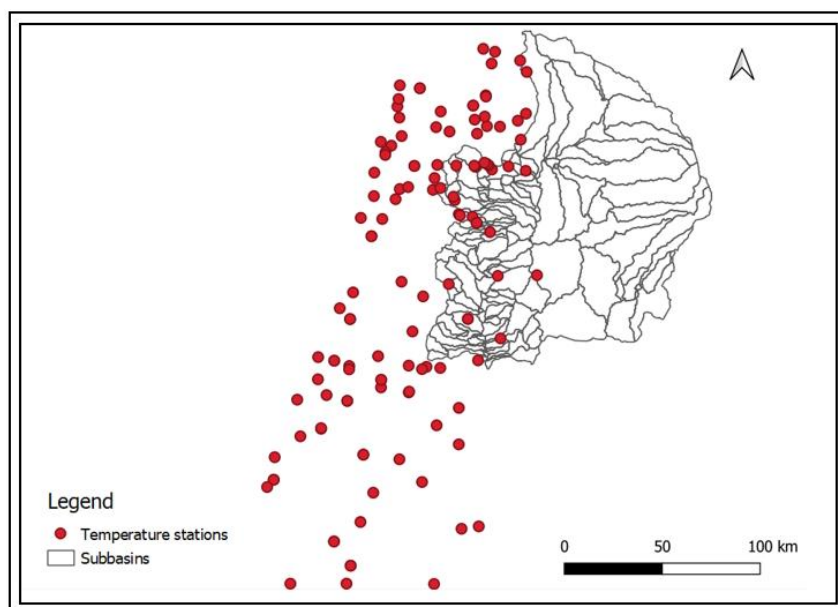


Figure 6. Available Temperature Stations

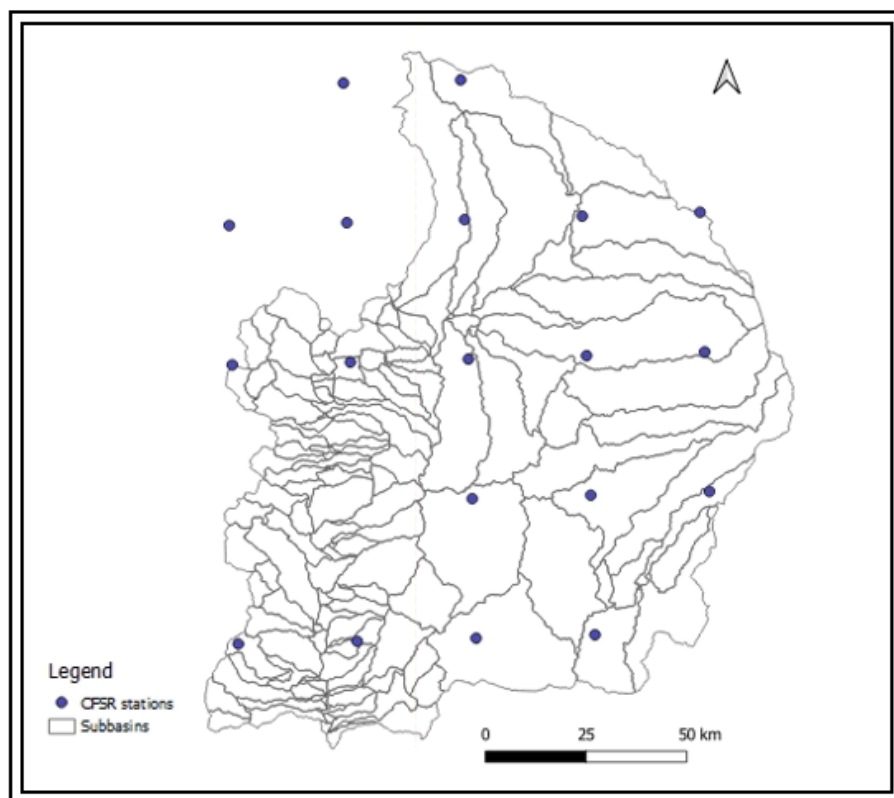


Figure 7. Available CFSR stations

The geospatial data necessary for the model setup includes the DEM, LULC, and Soil Type. Digital Elevation Model (Figure 8) sourced from the Shuttle Radar Topography Mission (SRTM GL1) Global 30m, providing high-resolution elevation data. Land Use (LU) information is obtained from the FAO GLC-SHARE (Global Land Cover SHARE) (Figure 9), which offers comprehensive land cover data. Soil data is derived from the Harmonized World Soil Database version 2.0 (HWSD v2.0) (Figure 10), ensuring detailed and harmonized soil information worldwide.

The land use and soil data provide a detailed overview of the area's utilization and soil types. Regarding land use (Table 2), agricultural land (AGRL) is the most prevalent, covering 52% of the area. Shrubland (SWRN) follows with 25%, and barren land (BARR) makes up 14%. Pastureland (PAST) covers 5%, while forested land (FRST) constitutes 2%. Urban high-density areas (URHD) represent 1% of land use. No land is allocated for rangeland (RNGB) or wetlands (WETW).

Regarding soil distribution (Table 3), the most common soil type is s3501, which covers 26.27% of the area. Other significant soil types include s3571 at 21.51%, s3534 at 14.89%, and s3135 at 11.78%. Urban land accounts for 4.08% of the area, while soils such as s3532 (4.72%), s3560 (4.97%), and s6687 (6.63%) are also present. Smaller areas are occupied by soils like s3502 (3.84%), s3612 (1.09%), s3133 (0.17%), s3586 (0.02%), s3322 (0.01%), and water (WATR) at 0.02%.

The watershed of Jordan Valley contains 8 active dams, Wehdah Dam (Yarmouk), Wadi Al-Arab Dam, Ziqlab Dam, Kufranja Dam, King Talal Dam, Al Karamah Dam, Shueib Dam, and Kafraïn Dam (Figure 11). Figure 12, presents the annual dams inflows for 2017-2022.

The hydrologic system in Jordan is heavily modified and the hydrologic data obtained are limited for the calibration of the inflow and outflow from the dams and their contribution to the Jordan River. A brief description of the function of the dams in Jordan follows.

- **Wehdah (or Unity) dam (Yarmouk)** - Wehdah Dam, with a storage capacity of 110.0 MCM, is a significant water source for irrigation and domestic use, particularly for supplying water to Amman via the King Abdullah Canal (KAC). Over the years, its production has fluctuated, starting at 39.2 MCM in 2014 and peaking at 93.7 MCM in 2017. In 2018, the dam produced 80.4 MCM. The dam supplies water to the north KAC.
- **Wadi Al-Arab dam** - Wadi Al Arab Dam has a storage capacity of 16.8 MCM and serves both irrigation and domestic water needs for Amman via the KAC. The water stored in the dam in the winter is then returned to the KAC during the summer. The reservoir water is used to irrigate about 12,500 dunums in the Northern Jordan Valley (namely around the area of North Shouneh and Al Baqura). It also serves as a drinking water source for the city of Amman in periods of water shortage through KAC. The dam's production started at 16.9 MCM in 2014 and decreased to 10.0 MCM by 2018, with annual variations in between.
- **Zeglab (or Ziglab) dam** - Ziglab Dam, with a capacity of 4.0 MCM, is primarily used for irrigation in the North Jordan Valley (12,500 dunums) and supplies water to KAC depending on availability. Its production has seen a decline from 1.8 MCM in 2014 to 0.8 MCM in 2018, with the lowest recorded production being 0.4 MCM in 2017.

- **Kufranja dam** -\_Kufrinjah Dam has a storage capacity of 7.8 MCM and is utilized for irrigation in the North Jordan Valley. Production data for this dam started to be recorded in 2017, with 1.2 MCM, and increased to 2.0 MCM in 2018.
- **King Talal Dam** - The water that originates from the King Talal Dam (KTD) is used for [irrigation](#) in the Jordan Valley (82,000 dunums in the middle Jordan Valley). KTD water is a mixture of treated wastewater and precipitation. It is transferred to KAC (South), downstream of the point where fresh water in the KAC is pumped to Amman for drinking. King Talal Dam, which boasts a storage capacity of 75.0 MCM, is a crucial source for irrigation in the South Jordan Valley. This dam had a high and relatively stable production over the years, starting at 123.0 MCM in 2014 and reaching a peak of 141.8 MCM in 2017 before slightly decreasing to 130.0 MCM in 2018
- **Wadi Shueib (or Shuaib) dam** -\_Wadi Shueib is in the Salt Valley of Jordan, a tributary watershed of the Jordan River. The city of Salt sits at the headwaters, and during the summer months the municipal sewage of Salt makes up a large portion of the Shueib's flows. In addition to base and floods flows, this dam now receives irrigation return flows and the effluent of the city of Salt WWTP. Fresh spring water in Wadi Shueib has declined to comply with the increasing drinking water demand. The flow was replaced by the effluent of WWTPs, a process that changed the ecological balance over time. Shueib dam is not connected to KAC; it is used for local irrigation (2500 dunums) in its vicinity. With a storage capacity of 1.7 MCM, Shuayb Dam is used for managed aquifer recharge (MAR) and irrigation in the South Jordan Valley. Its production has been relatively stable, fluctuating between 6.2 MCM in 2014 and 7.2 MCM in 2018.
- **Kafrein (or Kafrain) dam** - Kafrein Dam, which has a storage capacity of 8.5 MCM, serves irrigation needs in the South Jordan Valley. Its production increased from 10.1 MCM in 2014 to 15.4 MCM in 2015, with slight variations in the following years, resulting in a production of 9.9 MCM in 2018. During and after the rainy events, floodwater drains down to the Jordan River. It is not connected to KAC; instead, it used to irrigate the Hisban-Kafrein area (1,247 dunums).
- **Karameh (or Karama or Karamah) dam** -\_KAC South provides water to farmers, as well as to the newly constructed Karama Dam which stores winter water. In the summer the King Talal Dam and the Karama Dam supply KAC South. Karameh Dam has a storage capacity of 55.0 MCM but is not currently used for any specific purpose, with a total dissolved solids (TDS) concentration of 20 g/l. Its production varied, peaking at 6.2 MCM in 2017, but dropped significantly to 0.8 MCM in 2018.

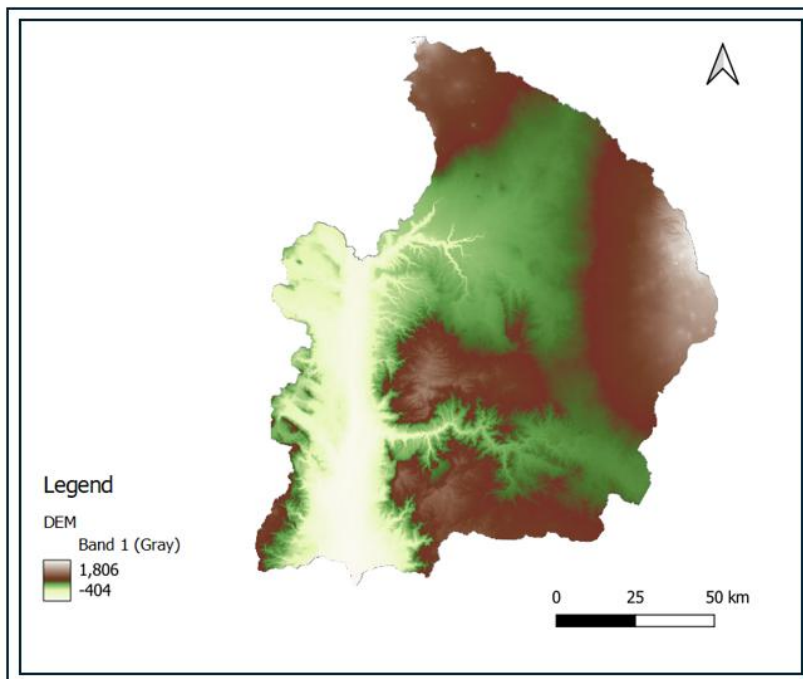


Figure 8. DEM of case study

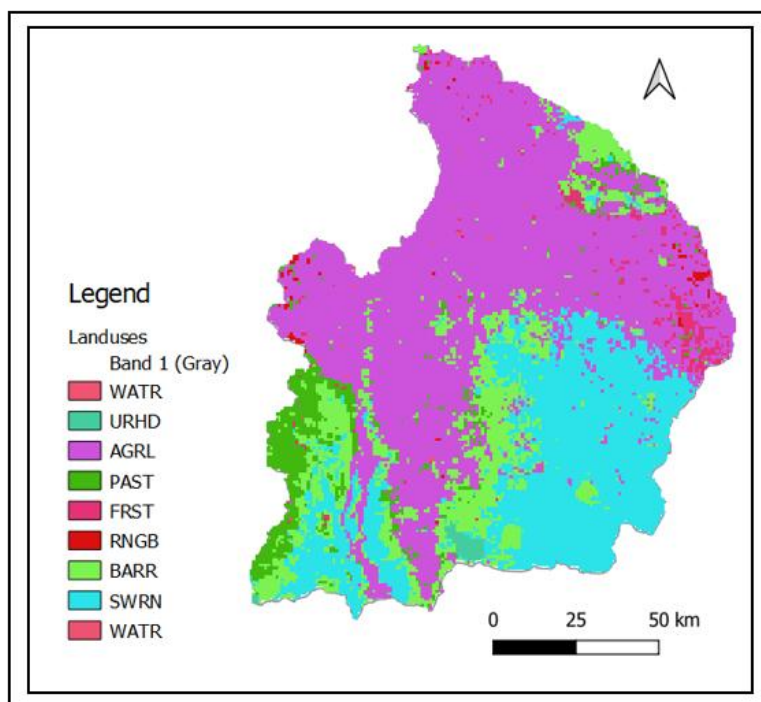


Figure 9. Soil Type of case study

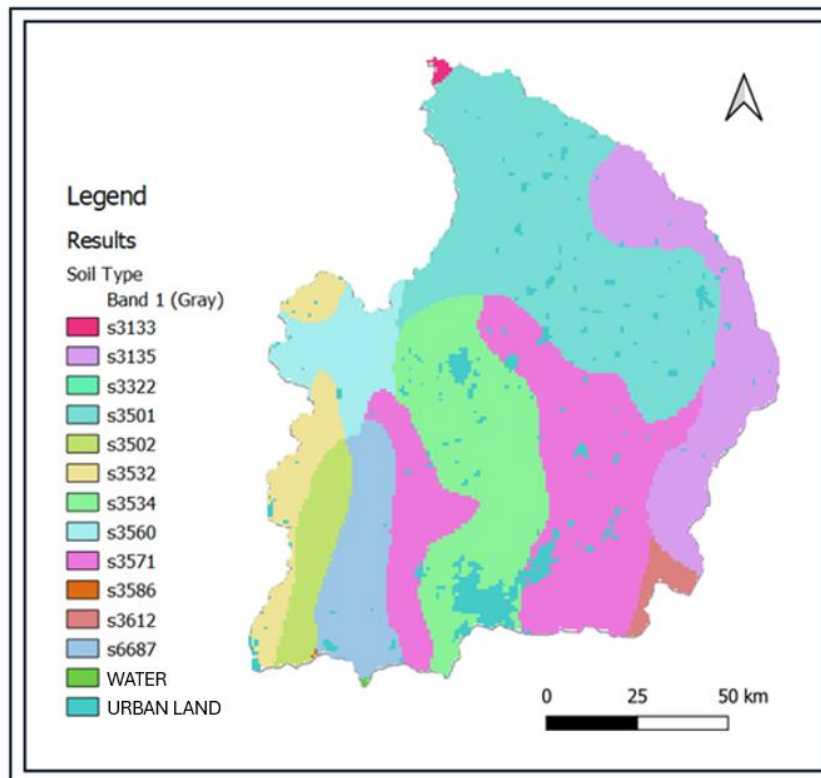


Figure 10. Land Uses of case study

Table 2. Percent Land Use Categories

Landuse	Percentage of Area
BARR	14%
AGRL	52%
FRST	2%
PAST	5%
RNGB	0%
WETW	0%
SWRN	25%
URHD	1%

Table 3. Soil Types and Their Respective Percentages

Soil Type	Percentage of Area
s3133	0.17%
s3501	26.27%
URBAN LAND	4.08%
s3322	0.01%
s3135	11.78%
s3534	14.89%
s3571	21.51%
s3532	4.72%
s3560	4.97%
s6687	6.63%
s3502	3.84%
s3612	1.09%
s3586	0.02%
WATR	0.02%

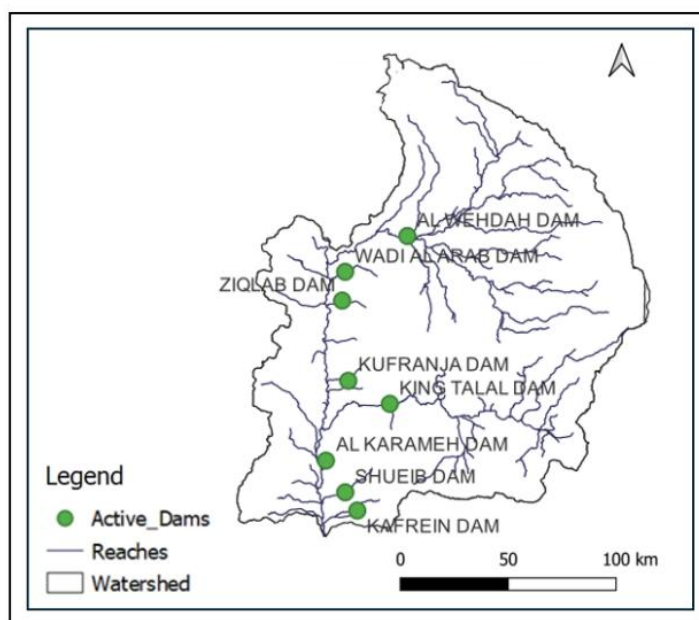


Figure 11. Available Dams in the case study

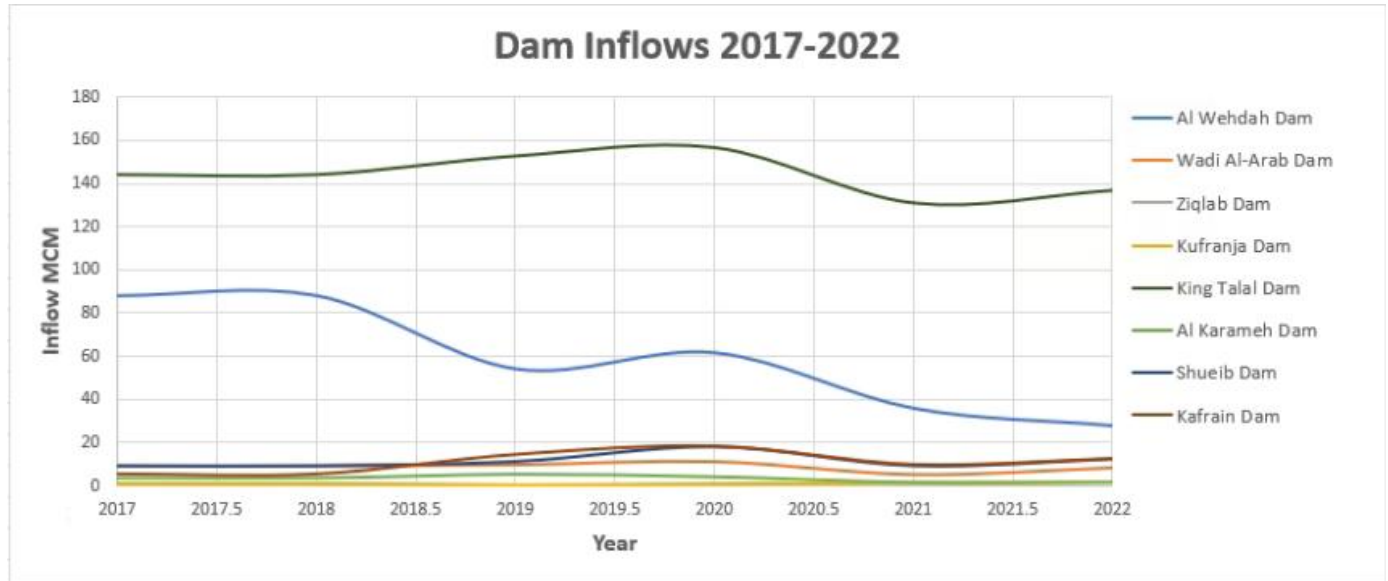


Figure 12. Fluctuation of the annual inflow of the dams (MCM)

Since the locations of the dams are given, along with the information that there are no dam outflows, we can restrict the simulation area to the sub-basins downstream of the dams, as shown in Figure 13. The final model setup consists of 61 sub-basins downstream of the dams.

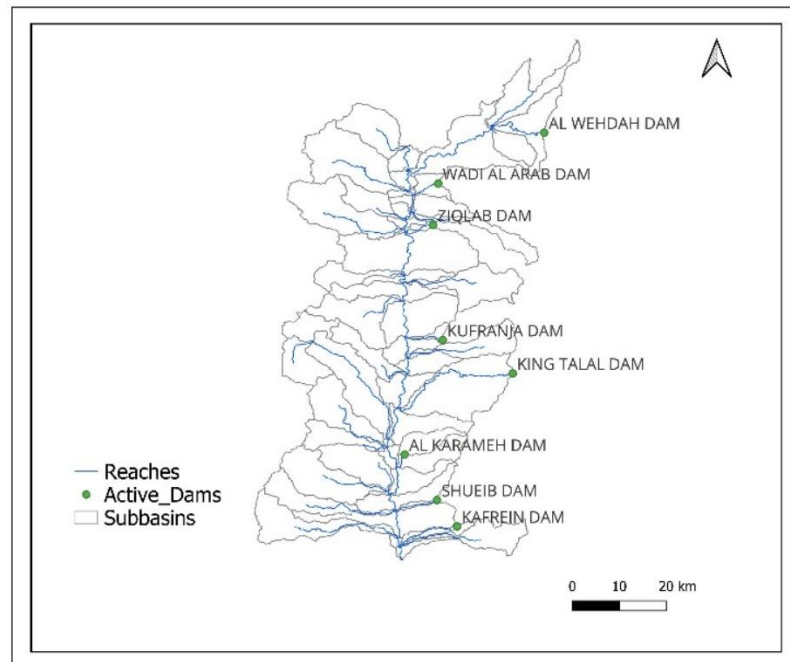


Figure 13. Model setup with subbasins and available Dams in the case study

## 2.2 Methodology

The first step in the modeling process is the collection of precipitation, meteorological, and hydrological station data. Precipitation and meteorological time series are used as input data for the model, while hydrometric station data and dam discharge information serve as field data for model calibration. Given the availability of hydrometric and meteorological data, the time period from 2000 to 2021 was simulated. Precipitation stations were selected based on the following criteria:

- Available data for 2000-2021
- Maximum distance of 40 km from watershed boundaries
- No data gaps during the 2000-2021 period

The percentage of data loss for precipitation is significantly lower than that for temperature due to the greater variability of precipitation compared to temperature. Temperature stations were mainly selected based on their proximity to the basin. Figures 14 and 15 present the stations of precipitation and temperature that satisfy the above criteria, while Tables 4 and 5 show the location of the precipitation and temperature stations used as input data in the simulation.

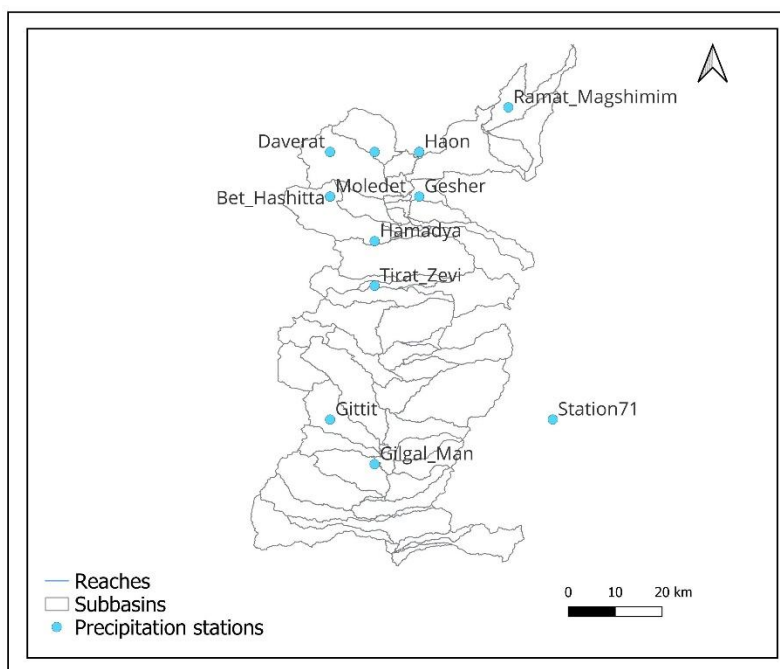


Figure 14. Selected Precipitation Stations

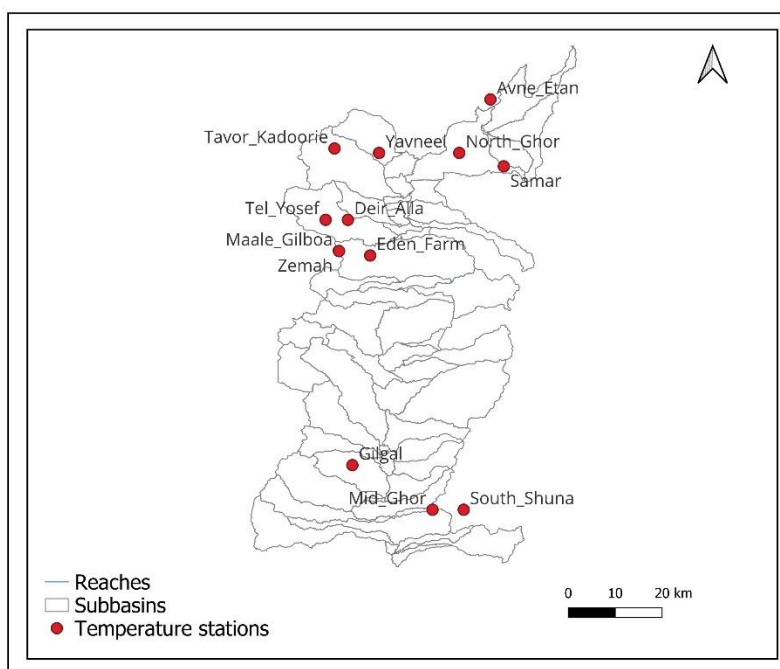


Figure 15. Selected Temperature Stations

Table 4. Characteristics of selected precipitation stations

Station Name EN	Latitude	Longitude	Institution
<b>Ashdot Yaaqov Meuhad</b>	32.664	35.582	IMS
<b>Bet Hashitta</b>	32.551	35.442	IMS
<b>Daverat</b>	32.646	35.351	IMS
<b>Gesher</b>	32.619	35.553	IMS
<b>Gilgal Man</b>	31.997	35.451	IMS
<b>Gittit</b>	32.101	35.396	IMS
<b>Hamadya</b>	32.520	35.521	IMS
<b>Haon</b>	32.728	35.625	IMS
<b>Moledet</b>	32.587	35.442	IMS
<b>Ramat Magshimim</b>	32.845	35.811	IMS
<b>Station 71</b>	32.125	35.875	CHRS
<b>Tirat Zevi</b>	32.422	35.526	IMS
<b>Yavneel Man</b>	32.703	35.505	IMS

Table 5. Characteristics of selected temperature stations

Station Name EN	Latitude	Longitude	Institution
Avne Etan	32.817	35.762	IMS
Eden Farm	32.468	35.489	IMS
Gilgal	31.997	35.451	IMS
Maale Gilboa	32.481	35.415	IMS
Tavor Kadoorie	32.705	35.407	IMS
Tel Yosef	32.546	35.395	IMS
Yavneel	32.698	35.510	IMS
Zemah	32.702	35.584	IMS
Deir Alla	32.192	35.619	NARC
Mid Ghor	31.904	35.625	NASA
North Ghor	32.696	35.692	NASA
Samar	32.674	35.785	WAJ
South Shuna	31.900	35.700	WAJ

### 2.2.1 Model Calibration and Sensitivity Analysis

The hydrologic system of the Jordan Valley is heavily modified with many reservoirs, canals and pumping stations that divert water for irrigation and drinking water supply. Daily time series of flow data for the inflow and outflow from the reservoirs are not available. Especially for the Yarmouk River, many dams are controlling the flow in Syria with no available data. In addition, the distribution of precipitation and meteorological stations is uneven with significant gaps. Finally, there are very few hydrometric stations in Jordan River and its tributaries with insufficient time series for proper hydrologic calibration of the area. Furthermore, the presence of a complex and insufficiently documented management system for water availability and distribution in the study area, coupled with conflicting information regarding available water supplies and extractions, currently renders precise and detailed modeling of the area unattainable. The collection of data in all three territories became extremely difficult due to the ongoing war in Gaza.

Given the above limitations, the hydrologic calibration was conducted for the Jordan Valley area (after the Jordanian Dams) and the aim was to capture the flow patterns and quantity of the Jordan River before it enters the Dead Sea and establish an average hydrologic budget for the JV.

The calibration utilized eight points with available field outflow data in an average daily step (Figure 16). Table 6 presents the calibration points' annual flow in million cubic meters (MCM). At the Yavneal station, data is available from 2013-2019, and the average annual runoff is 2.08 MCM. This measurement includes the addition of a small amount of water from aquaculture. The average annual flow for the Jordan Near Old Bridge station for 2013-2017 is 59.55 MCM, for the "Tavor-Betshean Tsemah Road" station for 2011-2015 is 0.69 MCM, and for the "Jordan Baptism Site" station for 2012-2021 is 118.63 MCM. The Harod station has an average annual outflow of 7.52 MCM for 2000-2021, which contains the amount of water

released by aquaculture farms. Water release into the river is permitted only for three months a year during the winter, from October 15th to January 15th.

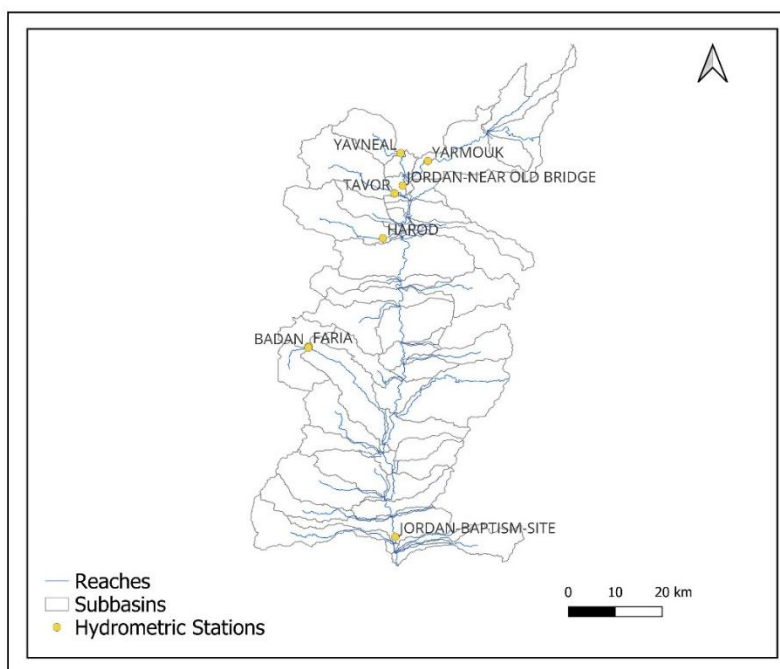


Figure 16. Calibration points

We performed a sensitivity analysis for each sub-basin using SWAT-CUP (SWAT Calibration and Uncertainty Programs), which links SUFI-2, PSO, GLUE, ParaSol, and MCMC methods to SWAT. We applied the Sequential Uncertainty Fitting algorithm (SUFI-2) (Abbaspour et al., 2004; 2007), which efficiently identifies optimal parameter ranges with relatively few model runs. SUFI-2 combines Latin Hypercube Sampling (LHS), multiple regression, and statistical ranking to conduct global sensitivity analysis. It samples hundreds of parameter sets from user-defined ranges using LHS, ensuring broad and uniform coverage of the parameter space. Each set is used to run SWAT, and model outputs (e.g., streamflow) are compared to observations using performance metrics. In our case, we used PBIAS to evaluate simulation accuracy in terms of streamflow quantity, aiming to identify which parameters most influence volumetric bias. After all runs, SUFI-2 performs multiple linear regression to relate parameter values to performance, calculating t-statistics (for ranking sensitivity) and p-values (for significance testing). We tested the 22 most influential parameters (Table 7), allowing them to vary within  $\pm 90\%$  of their baseline values, and ran 660 simulations per sub-basin with observed data.

Table 6. Annual flow in million cubic meters (MCM) of calibration points

YEAR	YAVNEAL	YARMOUK	JORDAN- NEAR OLD BRIDGE	TAVOR - BETSHEAN TSEMAH ROAD	HAROD - BET SHE'AN	FARIA	BADAN	JORDAN- BAPTISM SITE
2000		5.7			15.37			
2001		35.2			17.96			
2002		50.5			5.14			
2003		491.9			6.64			
2004		192.7			1.71			
2005		54.3			1.7	1.67	3.73	
2006		35.8			3.33	0.52	3.10	
2007		34.9			14.89	0.12	4.93	
2008		33.3			10.8			
2009		44.5			7.04			
2010		29.6			15.63			
2011		40.9		2.31	15.38			
2012		65.2			13.07			93.97
2013	1.09	75.9	73.56		8.04			156.37
2014	1.36	35.7	78.06		1.82			83.40
2015	3.15	36.2	67.37		4.86			103.97
2016	3.31	38.4	49.82		7.68			83.08
2017	0	35.5	28.95		3.87			61.82
2018	2.06	29.3			2.69			103.49
2019	3.59	75.6			4.21			160.08
2020					3.11			235.16
2021					0.52			104.93
Average	2.08	72.1	59.55	2.31	7.52	0.77	3.92	118.63

Table 7 QSWAT parameters used for sensitivity analysis

Parameter	Explanation	Characterization
<b>ALPHA_BF.gw</b>	Baseflow alpha factor (days)	Groundwater-related parameter
<b>TRNSRCH.bsn</b>	Transmission losses (fraction)	Basin-level parameter
<b>GW_DELAY.gw</b>	Groundwater delay time (days)	Groundwater-related parameter
<b>CH_N2.rte</b>	Manning's n value for the main channel	Routing reach or channel parameter
<b>GWQMN.gw</b>	Threshold depth of water in the shallow aquifer for return flow to occur (mm)	Groundwater-related parameter
<b>RCHRG_DP.gw</b>	Deep aquifer percolation fraction	Groundwater-related parameter
<b>OV_N.hru</b>	Manning's n for overland flow	Hydrologic Response Unit (HRU) parameter
<b>GW_REVAP.gw</b>	Groundwater revap coefficient	Groundwater-related parameter
<b>ESCO.hru</b>	Soil evaporation compensation factor	Hydrologic Response Unit (HRU) parameter
<b>CH_K2.rte</b>	Effective hydraulic conductivity in main channel alluvium (mm/hr)	Routing reach or channel parameter
<b>ALPHA_BNK.rte</b>	Alpha factor for bank storage (days)	Routing reach or channel parameter
<b>SOL_AWC().sol</b>	Available water capacity of the soil layer (mm H <sub>2</sub> O/mm soil)	Soil layer-specific parameter
<b>CN2.mgt</b>	SCS runoff curve number	Management-related parameter
<b>SURLAG.bsn</b>	Surface runoff lag time (days)	Basin-level parameter
<b>LAT_TTIME.hru</b>	Lateral flow travel time (days)	Hydrologic Response Unit (HRU) parameter
<b>SOL_Z().sol</b>	Depth from soil surface to bottom of layer (mm)	Soil layer-specific parameter
<b>SOL_K().sol</b>	Saturated hydraulic conductivity (mm/hr)	Soil layer-specific parameter
<b>SOL_BD().sol</b>	Moist bulk density (g/cm <sup>3</sup> )	Soil layer-specific parameter
<b>PLAPS.sub</b>	Precipitation lapse rate (mm/km)	Subbasin-level parameter
<b>TLAPS.sub</b>	Temperature lapse rate (°C/km)	Subbasin-level parameter
<b>CH_K1.sub</b>	Initial hydraulic conductivity of tributary channel (mm/hr)	Subbasin-level parameter
<b>CH_N1.sub</b>	Manning's n value for the tributary channels	Subbasin-level parameter

### 3. Results

Hydrologic calibration was performed for the following six stations:

**Yavneal Hydrometric Station** - The observed and simulated daily flow data for the Yavneal Hydrometric Station show good agreement, especially during the years 2018 and 2019 (Figure 17), while there are some discrepancies during the peaks in 2014 and 2015, obviously due to precipitation data uncertainty. The RMSE (Root Mean Square Error) of the simulation is 0.26, which is satisfactory. The coefficient of determination ( $R^2$ ) is 0.88 for the annual values, with a slight underestimation of the simulation, reflecting a good correlation between the observed and simulated values.

The most influential parameters ( $p$ -value  $< 0.05$ ) in the Yavneal subbasin are the Curve Number ( $t = 22.04$ ,  $p = 0.00$ ) and the saturated hydraulic conductivity of the soil ( $t = 2.18$ ,  $p = 0.03$ ). This indicates that surface runoff and soil permeability are the dominant controls on streamflow generation in this subbasin, with groundwater and channel parameters having secondary influence.

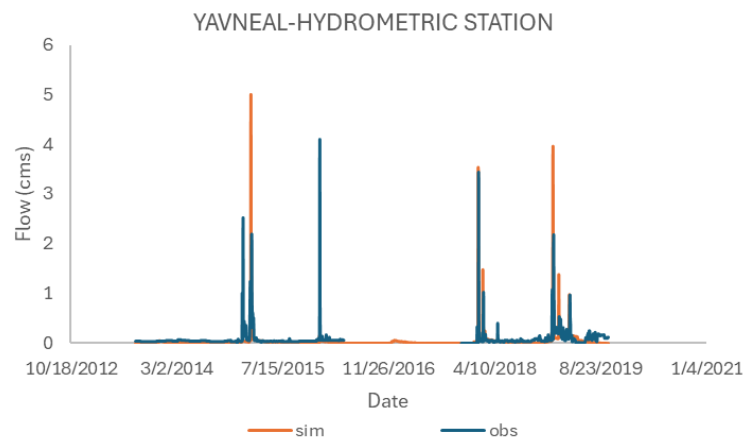


Figure 17. Comparison of observed and simulated daily flow data at the Yavneal hydrometric station.

**Jordan Near Old Bridge Hydrometric Station** - The simulation follows the observed daily data patterns for the Jordan Near Old Bridge Hydrometric Station, except for one high simulated peak (Figure 18). The RMSE of the simulation is 0.8 and the PBIAS is -0.9, suggesting that the model has a near-satisfactory performance in capturing the flow dynamics at this station. Notably, this station's time series is not typical and does not resemble the patterns of the flow in the rest of the subbasins.

The most influential parameters ( $p$ -value  $< 0.05$ ) in this subbasin are the channel hydraulic conductivity (CH\_K2,  $t = -20.24$ ,  $p = 0.00$ ), Manning's  $n$  for the main channel (CH\_N2,  $t = -8.68$ ,  $p = 0.00$ ), the depth of the soil layer (SOL\_Z,  $t = 2.99$ ,  $p = 0.00$ ), soil saturated hydraulic conductivity (SOL\_K,  $t = -2.68$ ,  $p = 0.01$ ), soil evaporation compensation factor (LAT\_TTIME,  $t = -2.68$ ,  $p = 0.01$ ), available water capacity

(SOL\_AWC,  $t = 2.61$ ,  $p = 0.01$ ), and the baseflow alpha factor (ALPHA\_BF,  $t = -2.23$ ,  $p = 0.03$ ). This indicates a dominant influence of both soil and channel parameters on streamflow in the Jordan near Old Bridge subbasin.

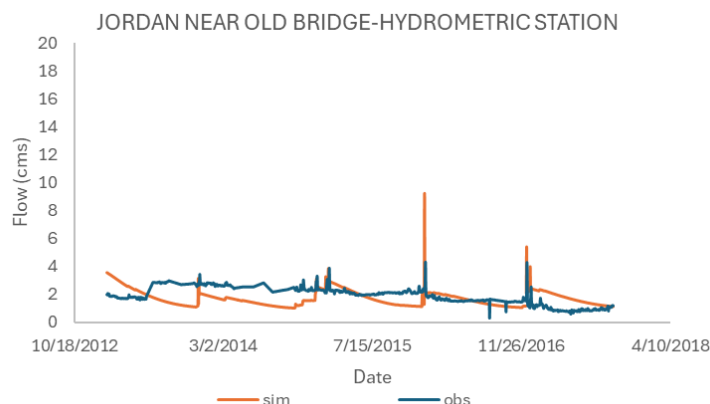


Figure 18. Comparison of observed and simulated daily flow data at the Jordan Near Old Bridge hydrometric station.

**Harod Hydrometric Station** - The Harod Hydrometric Station displays pronounced variability in observed streamflows, particularly during the winter months. This variability is largely attributed to regulated water discharges from aquaculture operations in the Harod and Beit She'an Valleys. As part of a national reform implemented to manage effluent water from fishponds, aquaculture farms are permitted to release treated water into the Harod Stream only between October 15th and January 15th each year. This seasonal discharge regime—mandated by environmental regulations requiring sedimentation treatment and compliance with water quality standards—introduces artificial peaks in streamflow during these months, which are not always captured in baseline hydrological simulations

To tackle this, we ‘simulate’ these discharges by introducing point sources in the Harod subbasin as well as in the main stream, downstream of Harod. The specific quantities that enter are unknown and we can only approximate them. Specifically, 67 Mm<sup>3</sup>/yr are introduced to Israel through Harod and the main streamflow. Based on the modeling of the nearby Yavneal basin, almost half of the water goes away through evapotranspiration, leaving 33 Mm<sup>3</sup>/yr to be discarded in Harod and the main flow stream. This amount was estimated using the calculated potential evapotranspiration rate from the model and the areal extent of the fishing ponds in the area. To approximate the amount introduced as a point source in the Harod subbasin, we consider a percentage of the 33 Mm<sup>3</sup>/yr, divide it into the days of the period October 15<sup>th</sup> – January 15<sup>th</sup>, we examine the goodness of fit with the observations, and through trial and error we end up with the best goodness of fit (Figure 19). It is estimated that about 4 Mm<sup>3</sup>/yr are discarded through Harod and the rest 29 Mm<sup>3</sup>/yr are discarded in the main streamflow (we add a point source in the basin downstream to simulate these too).

The simulation for the monthly flow of Harod shows deviations from the observed data, particularly around 2007-2008, and 2012 (Figure 19), owing to the uncertainty of discharged water. Considering the uncertainty of the specific simulation, the metrics are very good, with PBIAS equal to 0.1, RMSE equal to 0.29, and NSE equal to 0.8.

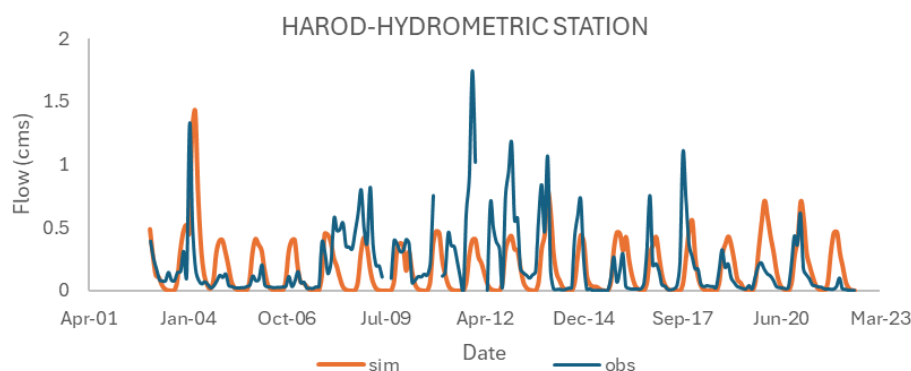


Figure 19. Comparison of observed and simulated monthly flow data at the Harod hydrometric station.

Based on the sensitivity analysis, the most significant parameters ( $p$ -value  $< 0.05$ ) are the Curve Number ( $t = 15.39$ ,  $p = 0.00$ ), the baseflow alpha factor ( $t = 2.14$ ,  $p = 0.03$ ), the soil bulk density ( $t = 2.17$ ,  $p = 0.03$ ), the soil depth ( $t = -3.55$ ,  $p = 0.00$ ), and the threshold depth of water in the shallow aquifer required for return flow ( $t = -6.55$ ,  $p = 0.00$ ). This suggests that the Harod basin's flow dynamics are strongly influenced by groundwater processes and soil physical properties.

**Tavor Hydrometric Station** - At the Tavor Hydrometric Station, the available data are limited (Figure 20). To calibrate the model for the specific subbasin we used the parameters from the nearby Harod, yielding a good RMSE of 0.3. The results of the sensitivity analysis for Tavor, coincide with the ones of Harod.

Based on the sensitivity analysis, the most influential parameters ( $p$ -value  $< 0.05$ ) in the Tavor subbasin are the Curve Number (CN2,  $t = 21.33$ ,  $p = 0.00$ ), bulk density of the soil layer (SOL\_BD,  $t = 3.22$ ,  $p = 0.00$ ), depth of soil layer (SOL\_Z,  $t = -2.92$ ,  $p = 0.00$ ), groundwater threshold for baseflow (GWQMN,  $t = -2.52$ ,  $p = 0.01$ ), and the available water capacity of the soil (SOL\_AWC,  $t = -2.32$ ,  $p = 0.02$ ). This suggests that in the Tavor subbasin, soil properties and groundwater storage thresholds are dominant controls on runoff quantity.

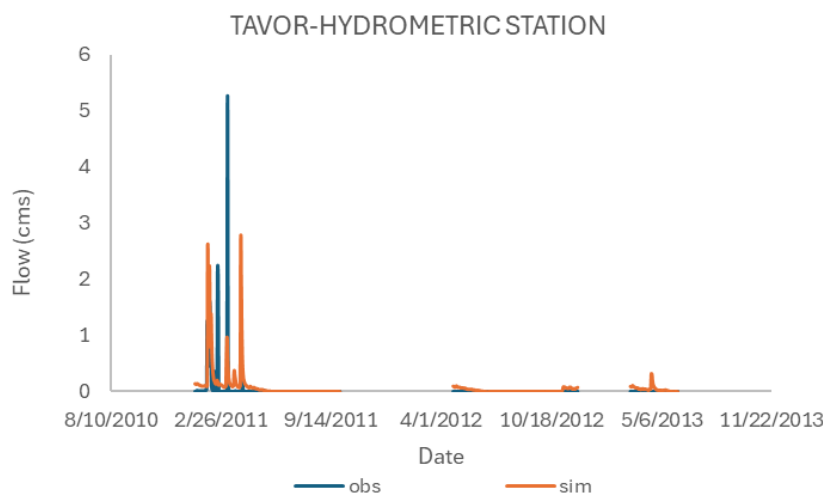


Figure 20. Comparison of observed and simulated daily flow data at the Tavor hydrometric station.

**Yarmouk Hydrometric Station** – The observational flow data for the Yarmouk hydrometric station yield two very high peaks (during 2003 and 2004) that cannot be attributed to the observational rainfall (Figure 21). These may be artifacts from the hydrometric station's measurements. The rest of the simulation follows the observations satisfactorily, with a good PBIAS of 0.13 and a near-satisfactory NSE of 0.3. When the two peaks are omitted, the NSE is satisfactory (0.74).

Based on the sensitivity analysis, the most influential parameters ( $p$ -value  $< 0.05$ ) in the Yarmouk basin are the Curve Number ( $t = 25.20$ ,  $p = 0.00$ ), the bulk density of the soil ( $t = 2.21$ ,  $p = 0.03$ ), and the bank storage recession coefficient ( $t = -2.10$ ,  $p = 0.04$ ). These results suggest that runoff generation and soil physical characteristics play a dominant role in controlling streamflow dynamics in the Yarmouk basin.

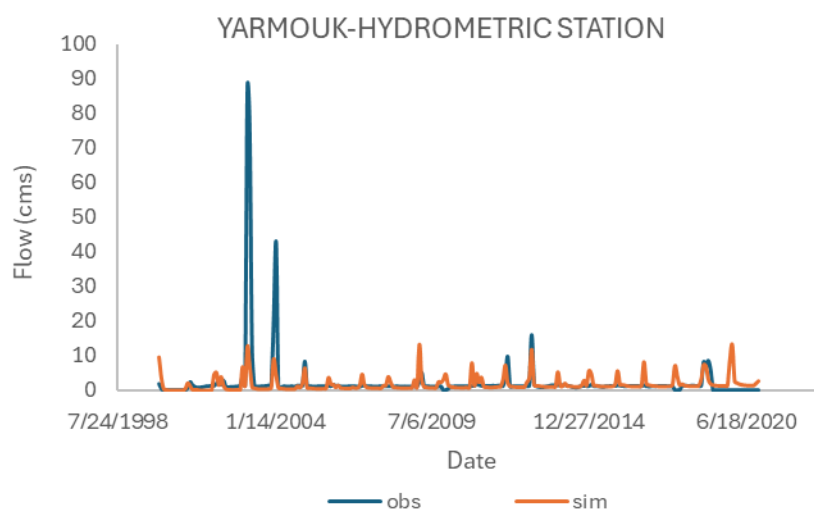


Figure 21. Comparison of observed and simulated monthly flow data at the Yarmouk hydrometric station.

**Faria Hydrometric Station** – The framework followed for calibration for the subbasins extending downwards from Faria was: (1) calibration of flow in the subbasin of Faria achieving the best goodness of fit possible, (2) transferring of the calibrated parameter set to Badan and the rest of the subbasins downstream, including the Jordan Baptism Site near the exit. The daily flow simulation for Faria yielded good PBIAS (-0.07) and RMSE (0.09) indices and was successful for the hydrological year 2005-2006, while it underestimated and overestimated, respectively, the flow in the hydrological years 2004-2005 and 2006-2007 (Figure 22).

Based on the sensitivity analysis, the most significant parameters ( $p$ -value  $< 0.05$ ) are the Curve Number ( $t$ -value = 31.24,  $p$ -value = 0.00), the precipitation lapse rate ( $t$ -value = -5.06,  $p$ -value = 0.00), the depth of the soil layer ( $t$ -value = -3.70,  $p$ -value = 0.00), and the soil bulk density ( $t$ -value = 2.23,  $p$ -value = 0.03). These results suggest that streamflow in the Faria sub-basin is primarily influenced by precipitation distribution and soil physical properties, particularly those controlling infiltration and retention.

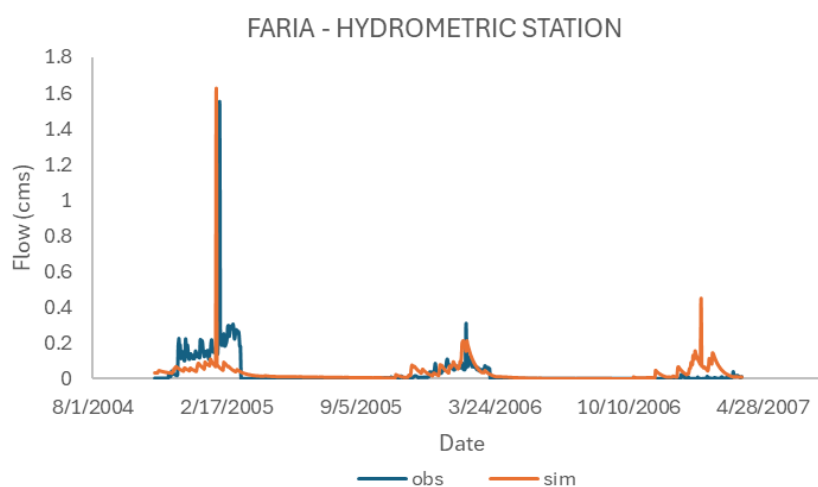


Figure 22. Comparison of observed and simulated daily flow data at the Faria hydrometric station.

**Badan Hydrometric Station** – Following the calibration strategy of Faria, the daily flow simulation for Badan is excellent for the hydrologic year 2004-2005 and satisfactory for 2006-2007, but the simulation fails to capture the peak during 2005-2006 (Figure 23). This issue is owed to the precipitation station attributed to Badan which has not captured realistically the local precipitation during this year. Nevertheless, the calibration has a good RMSE (0.26) and near to satisfactory PBIAS (0.37).

Based on the sensitivity analysis, the most significant parameters ( $p$ -value  $< 0.05$ ) are the Curve Number ( $t$ -value = 22.32,  $p$ -value = 0.00), the initial channel hydraulic conductivity (CH\_K1) ( $t$ -value = -5.57,  $p$ -value = 0.00), the precipitation lapse rate ( $t$ -value = -5.56,  $p$ -value = 0.00), the soil bulk density ( $t$ -value = 5.25,  $p$ -value = 0.00), the available water capacity of the soil layer ( $t$ -value = -3.14,  $p$ -value = 0.00), and the channel Manning's  $n$  value (CH\_N1) ( $t$ -value = -2.22,  $p$ -value = 0.03). These results indicate that the hydrologic response of the Badan sub-basin is primarily influenced by soil properties and channel flow characteristics.

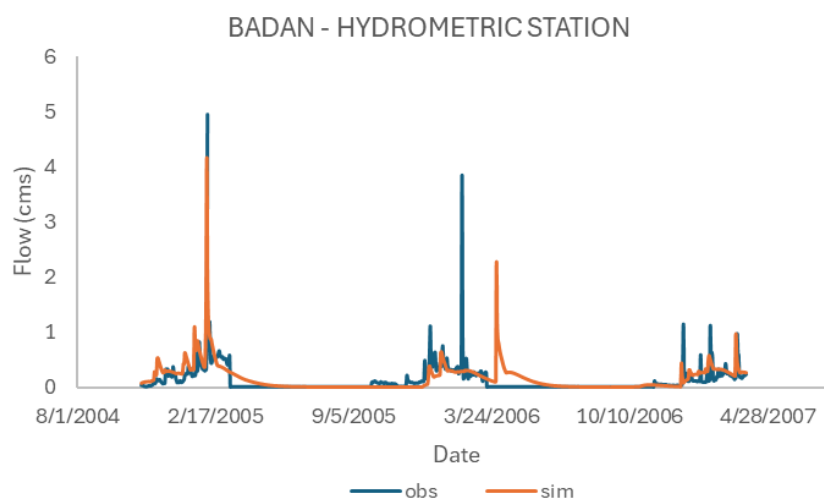


Figure 23. Comparison of observed and simulated daily flow data at the Faria hydrometric station

**Jordan Baptism Site Hydrometric Station** – The calibration of the model at the Jordan Baptism Site was informed by the parameterization of two upstream subbasins with the most reliable hydrometric records: Faria and Badan. The same set of calibrated parameters was applied to all intermediate subbasins located between Faria, Badan, and the Jordan Baptism Site. The strong agreement between observed and simulated streamflow at the Jordan Baptism Site—a hydrometric station situated near the basin outlet—demonstrates the robustness of the upstream calibration and lends credibility to the model results for the lower part of the watershed (Figure 24), with some overestimations and underestimations at times, leading however to an excellent PBIAS (0.009), a satisfactory R2 of 0.38, and an NSE of 0.17. On an annual scale, the model captures the flow variations very well (Figure 25) with excellent PBIAS (0.02), NSE (0.92), and satisfactory R2 (0.52) indices.

For the estimation of the sensitivity of the flow simulation near the exit, we have to consider all subbasins contributing to the flow. Results suggest that the most influential parameters ( $p$ -value < 0.05) are the Curve Number (t-value = 16.37,  $p$ -value = 0.00), the transmission loss coefficient (TRNSRCH) (t-value = -9.39,  $p$ -value = 0.00), the channel hydraulic conductivity (CH\_K2) (t-value = -7.70,  $p$ -value = 0.00), the soil depth (SOL\_Z) (t-value = -2.41,  $p$ -value = 0.02), and the channel Manning's  $n$  value (CH\_N2) (t-value = -2.77,  $p$ -value = 0.01). These findings indicate that the outflow at the Jordan Baptism Site is primarily governed by surface runoff generation, channel transmission losses, and in-stream flow resistance, integrating the effects of all upstream sub-basins.

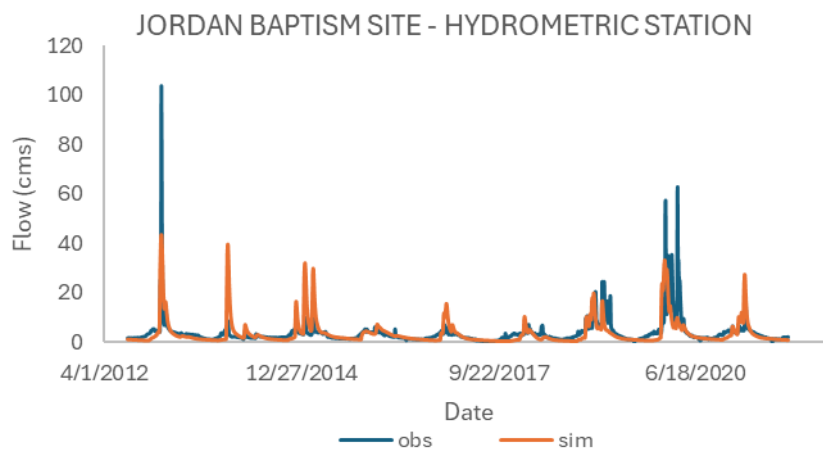


Figure 24. Comparison of observed and simulated daily flow data at the Jordan Baptism Site hydrometric station.

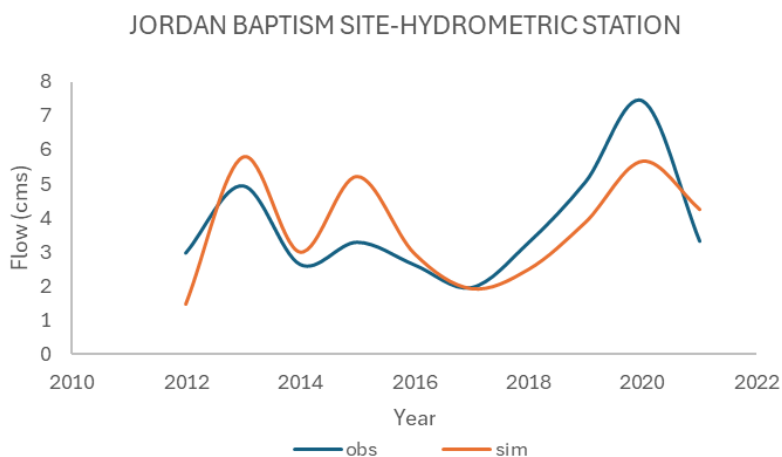


Figure 25. Comparison of observed and simulated annual flow data at the Jordan Baptism Site hydrometric station

The results of the sensitivity analysis are summarized in Table 8, where the most significant variables along with their p-values ( $<0.05$ ) and t-values are shown. The Curve Number is a key calibration parameter basin-wide and must be prioritized in any regional management scenario. Soil parameters (SOL\_Z, SOL\_AWC, SOL\_BD) are dominant in the north and west, linking infiltration and soil moisture dynamics to streamflow. Channel routing parameters (CH\_K2, CH\_N2, CH\_K1) become more significant downstream, especially at outlet stations. Finally, the Jordan Baptism Site, being downstream, captures integrated sensitivity and exhibits significance across the broadest parameter set

Table 8. T-values (p-values) of the most significant parameters (p-value < 0.05) from the sensitivity analysis of every sub-basin with available hydrological data

Parameter	Yavneal	Jordan Old Bridge	Harod	Tavor	Yarmouk	Faria	Badan	Jordan Baptism Site
CN2.mgt	22.04 (0.00)	16.37 (0.00)	15.39 (0.00)	21.33 (0.00)	25.20 (0.00)	31.24 (0.00)	22.32 (0.00)	16.37 (0.00)
SOL_K(..).sol	2.18 (0.03)	-2.68 (0.01)						
CH_K2.rte		-20.24 (0.00)						-7.70 (0.00)
CH_N2.rte		-8.68 (0.00)						-2.77 (0.01)
SOL_Z(..).sol		-2.99 (0.00)	-3.55 (0.00)	-2.92 (0.00)		-3.70 (0.00)		-2.41 (0.02)
LAT_TTIME.hru		-2.68 (0.01)						
SOL_AWC(..).sol		-2.61 (0.01)		-2.32 (0.02)			-3.14 (0.00)	
ALPHA_BF.gw		-2.23 (0.03)	2.14 (0.03)					
GWQMN.gw			-6.55 (0.00)	-2.52 (0.01)				
SOL_BD(..).sol			2.17 (0.03)	3.22 (0.00)	2.21 (0.03)	2.23 (0.03)	5.25 (0.00)	
CH_K1.sub							-5.57 (0.00)	
CH_N1.sub							-2.22 (0.03)	
PLAPS.sub						-5.06 (0.00)	-5.56 (0.00)	
TRNSRCH.bsn					-2.10 (0.04)			-9.39 (0.00)

Table 9 presents the simulated flows and observed flows in MCM for each year. Table 10 shows the variability of weighted average precipitation and evapotranspiration (ET) in the Jordan Valley from the year 2000 to 2021. The average annual precipitation over this period is 299.8 mm, with a minimum of 124.7 mm in 2017 and a maximum of 399.6 mm in 2003. On the other hand, the average annual ET is 203.3 mm, with values ranging from 154.2 mm in 2017 to a peak of 272.2 mm in 2020. When estimating the trend in the Western and Eastern part of the basin, there is a slight increase in the rainfall of the western part of the basin during the 21 years of analysis but a twice the magnitude decrease in the eastern part of the basin. The variability is also presented in Figure 26 and Figure 27. Figure 28 presents the Outflow of the Jordan River in mm per year which exhibits a declining trend during the 21 years of analysis.

Table 9. Comparison of observed and simulated flow in MCM of calibration points.

Year	YAVNEAL OBS	YAVNEAL SIM	YARMOUK OBS	YARMOUK SIM	J.N.OB. OBS	J.N.O.B. SIM	TAVOR OBS	TAVOR SIM	HAROD OBS	HAROD SIM	FARIA OBS	FARIA SIM	BADAN OBS	BADAN SIM	JORDAN- BAPTISM SITE OBS	JORDAN- BAPTISM SITE SIM
2001			35.18	23.31												
2002			50.46	53.72					5.14	4.89						
2003			491.90	68.55					6.64	14.92						
2004			192.69	52.15					1.71	4.70						
2005			54.33	46.50					1.70	4.43	1.67	1.01	3.73	5.57		
2006			35.77	29.77					3.33	4.65	0.52	0.80	3.10	4.02		
2007			34.94	40.99					14.89	4.63	0.12	1.45	4.93	6.22		
2008			33.33	42.57					10.80	4.83						
2009			44.51	79.83					7.04	3.94						
2010			29.60	58.20					15.63	3.57						
2011			40.88	53.54			2.3	3.3	15.38	3.89						
2012			65.16	67.11			-		13.07	5.77					93.97	40.14
2013	1.09	0.23	75.93	76.25	73.56	62.96	-		8.04	7.11					156.37	205.79
2014	1.36	0.20	35.67	45.18	78.06	45.93	-		1.82	3.96					83.40	82.83
2015	3.15	1.28	36.22	60.94	67.37	58.90	-		4.86	6.17					103.97	165.79
2016	3.31	0.70	38.38	71.48	49.82	51.48			7.68	4.47					83.08	88.53
2017	0.00	0.01	35.47	42.47	28.95	54.02			3.87	4.41					61.82	56.16
2018	2.06	1.58	29.33	70.54					2.69	5.52					103.49	75.24
2019	3.59	2.74	75.65	100.14					4.21	7.86					160.08	126.74
2020									3.11	7.20					235.16	183.11
2021									0.52	3.59					104.93	135.24
Average	2.08	0.97	72.1	57.01	59.55	54.66	2.3	3.3	6.68	5.56	0.77	1.09	3.92	5.27	118.63	116.0

Table 10. Weighted average precipitation and potential evapotranspiration for each year.

Year	PRECIP (mm)	ET(mm)
2000	309.2	224.2
2001	248.5	180.6
2002	372.1	230.9
2003	399.6	238.4
2004	303.5	191.3
2005	256.3	187.6
2006	279.8	211.6
2007	274.4	205.7
2008	226.1	161.0
2009	347.7	218.0
2010	208.8	162.5
2011	306.3	233.1
2012	332.3	210.1
2013	344.8	189.3
2014	239.5	192.5
2015	353.4	228.2
2016	272.3	161.4
2017	124.7	154.2
2018	372.1	219.8
2019	340.0	217.4
2020	398.3	272.2
2021	284.9	182.4
<b>Average</b>	<b>299.8</b>	<b>203.3</b>

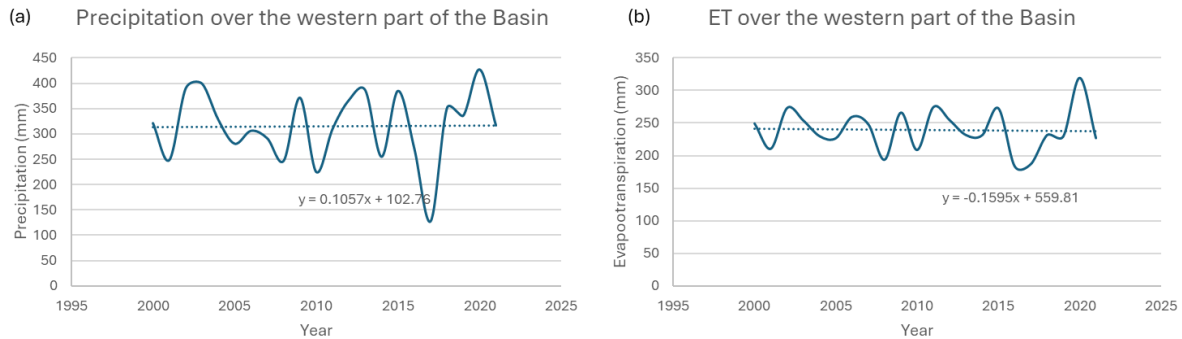


Figure 26. Variability of weighted average precipitation and evapotranspiration in the western Jordan Valley

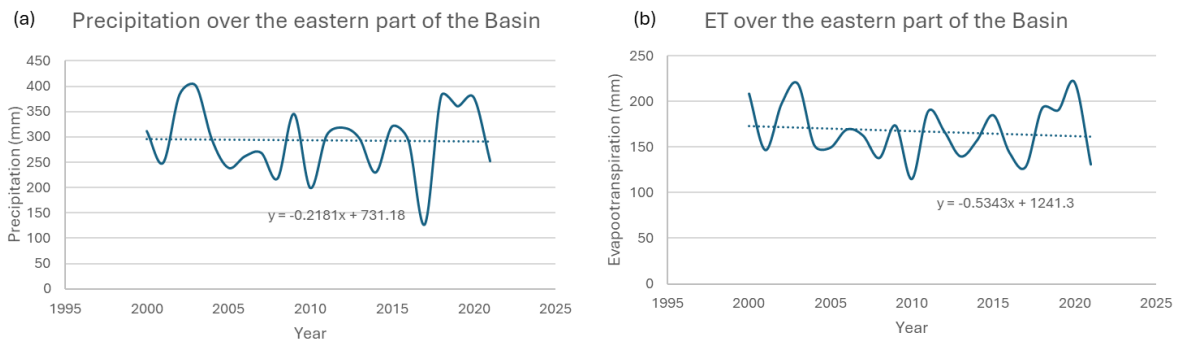


Figure 27. Variability of weighted average precipitation and evapotranspiration in the eastern Jordan Valley

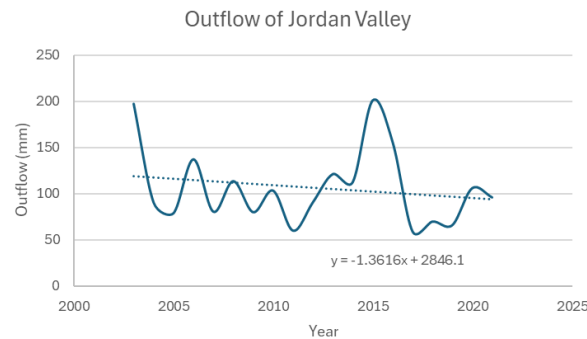


Figure 28. Average Annual Inflow and Outflow of the Jordan River for 2000-2021

**Hydrologic Budget** – Based on the hydrologic simulation for the years 2000-2021 the following hydrologic budget for the Jordan Valley was estimated. The total area simulated is 4225 km<sup>2</sup>, the annual average areal weighted precipitation was 290 mm and the annual average areal weighted ET 200 mm. This translates into 1225 Mm<sup>3</sup>/yr of precipitation volume and 845 Mm<sup>3</sup>/yr volume of ET. The available water is the difference 380 Mm<sup>3</sup>/yr of which 121 Mm<sup>3</sup>/yr is the average outflow of Jordan river to the Dead Sea. The pumping volumes from groundwater in the immediate JV (up to elevation of 200m) amount to 67 Mm<sup>3</sup>/yr in the Israeli section, 32 Mm<sup>3</sup>/yr in the Palestinian section and 47 Mm<sup>3</sup>/yr in the Jordanian section (total of 146 Mm<sup>3</sup>/yr). To these abstractions, we should add the pumping in Area C by Israel.

## 4. Conclusions

The hydrologic system of the Jordan valley is heavily modified with many reservoirs, canals and pumping stations that divert water for irrigation and drinking water supply. Heavily modified hydrologic systems require detailed daily time series of flow data for the inflow and outflow from the reservoirs as well as water abstractions and diversions which are not available for the Jordan Valley basin. Especially for the Yarmuk River, there are many dams controlling the flow in Syria with no available data. In addition, the distribution of precipitation and meteorological stations is uneven with significant gaps. Finally, there are very few hydrometric stations in Jordan River and its tributaries with insufficient time series for proper hydrologic calibration of the area.

The lack of available data as well as the presence of a complex and insufficiently documented management system for water availability and distribution in the study area, coupled with conflicting information regarding available water supplies and extractions, currently renders precise and detailed modeling of the area unattainable. The collection of data in all three territories became extremely difficult due to the ongoing war in Gaza.

Given the above limitations, the hydrologic calibration was conducted for the Jordan valley area (after the Jordanian Dams) and the aim was to capture the flow patterns and quantity of the Jordan River before it enters the Dead Sea and establish an average hydrologic budget for the JV.

Based on the hydrologic simulation for the years 2000-2021 the following hydrologic budget for the Jordan Valley was estimated. The total area simulated is 4225 km<sup>2</sup>, the annual average areal weighted precipitation was 290 mm and the annual average areal weighted ET 200 mm. This translates into 1225 Mm<sup>3</sup>/yr of precipitation volume and 845 Mm<sup>3</sup>/yr volume of ET. The available water is the difference 380 Mm<sup>3</sup>/yr of which 121 Mm<sup>3</sup>/yr is the average outflow of Jordan river to the Dead Sea. In addition, the groundwater abstraction has been estimated to 146 Mm<sup>3</sup>/yr in the three territories (not accounting for the pumping in area C of the Palestinian territory).

The available water resources in the JV are extremely limited and are expected to decline due to climate change with significant impact on the ecosystem and the biodiversity as well as the available water supply to cover the demand for drinking water and agriculture.

This hydrologic simulation will be used to simulate the sediment transport and nitrate concentrations in the surface and groundwater in the Jordan valley as part of the Ecosystem assessment that will be conducted in the EcoFuture project.

## References

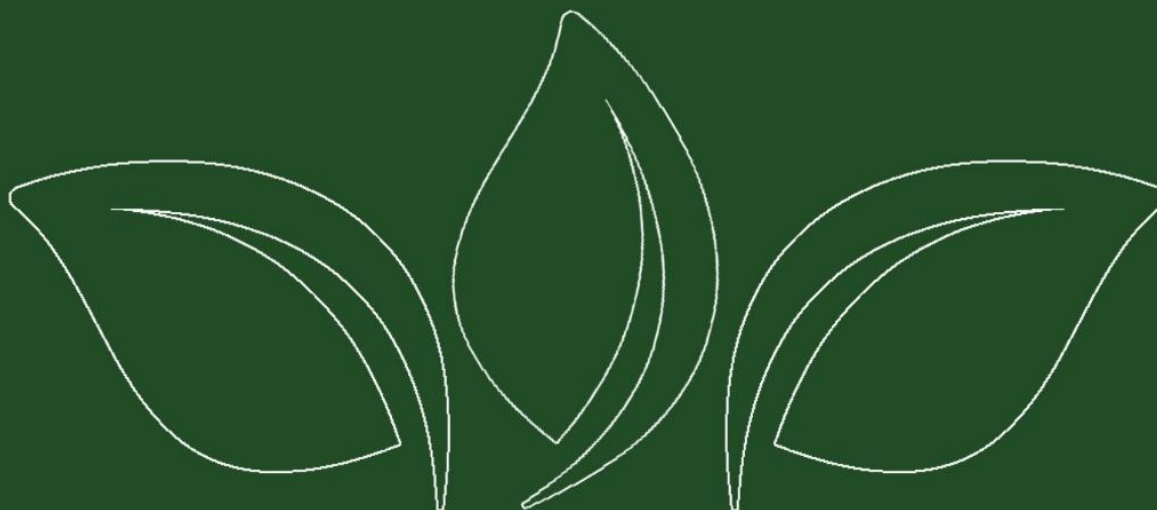
- Abbaspour, K.C., Johnson, C.A., and van Genuchten, M.T., 2004. Estimating Uncertainty of Model Predictions Using the Sequential Uncertainty Fitting Procedure (SUFI-2). *Vadose Zone Journal*, 3(4), 1340–1352.
- Abbaspour, K.C., 2007. User Manual for SWAT-CUP, SWAT Calibration and Uncertainty Analysis Programs. Eawag: Swiss Federal Institute of Aquatic Science and Technology, Duebendorf, 103 p
- Al Absi, K., Aburwaq, R., Dahabiyeh, M., Ershaid, M., Gharybeh, M., Al Hesa, H., Margane, A., Al Masri, M., Mikovec, R., Mufarih, M., Al Obeiaat, A., Shaheen, H., Uleimat, A., 2020. Rapid Assessment of the Consequences of Declining Resources Availability and Exploitability for the Existing Water Supply Infrastructure, Deutsche Gesellschaft für Internationale Zusammenarbeit (GIZ) GmbH and Ministry of Water and Irrigation (MWI), 1-365.
- Jreisat, K., Yazjeen, T., 2013. A Seismic Junction, In: *Atlas of Jordan*, Presses de l'Ifpo, 47-59. <https://doi.org/10.4000/books.ifpo.4861>
- Kool, J., 2016. The Jordan Valley, In: *Sustainable Development in the Jordan Valley*, Hexagon Series on Human and Environmental Security and Peace, Springer, 13, 1-237. [https://doi.org/10.1007/978-3-319-30036-8\\_2](https://doi.org/10.1007/978-3-319-30036-8_2)
- Royal HaskoningDHV, MASAR Center Jordan, 2015. National Master Plan for the Jordan River Valley, EcoPeace Middle East, 1-199.
- Suleiman, R., 2003. Water Resources Development in the Jordan River Basin in Jordan, In: *The 3rd conference of the International Water History association*, International Water Management Institute, 1-110.
- Tech, T., 2020. WATER MANAGEMENT INITIATIVE (WMI), National Water Infrastructure Master Plan, Intervention 4.4.2, USAID Jordan, 1-377.
- USAID/Jordan Water Innovations Technologies (WIT), 2018. Development of Groundwater Geospatial Database for Jordanian Highlands and Jordan Valley.

Zeitoun, M., Abdallah, C., Dajani, M., Khresat, S., Elaydi, H. and Alfarrar, A. 2019. The Yarmouk tributary to the Jordan River I: Agreements impeding equitable transboundary water arrangements. *Water Alternatives* 12(3): 1064-1094.

## Project Coordinator



## Project Partners



This publication reflects only the author's view and the PRIMA Foundation is not responsible for any use that may be made of the information it contains